

МІНІСТЕРСТВО ОСВІТИ І НАУКИ УКРАЇНИ
НАЦІОНАЛЬНИЙ АВІАЦІЙНИЙ УНІВЕРСИТЕТ

Факультет літальних апаратів

Кафедра авіаційних двигунів

ДОПУСТИТИ ДО ЗАХИСТУ

Завідувач кафедри

Докт.техн. наук , проф.

Терещенко Ю.М.

“ _____ ” _____ 2022 р.

ДИПЛОМНА РОБОТА

(ПОЯСНЮВАЛЬНА ЗАПИСКА)

ВИПУСКНИКА ОСВІТНЬО-КВАЛІФІКАЦІЙНОГО РІВНЯ

“МАГІСТР”

Тема: Заходи по підвищенню паливної ефективності силової

установки для дальньо-магістральних пасажирських

літаків

Виконавець: Пен Сяосін

Керівник: к.т.н., проф. Гвоздецький І. І.

Консультанти з розділів:

охорона праці: к.т.н., Кажан К. І.

охорона навколишнього

середовища: к.т.н. , доцент Павлюх Л.І.

Нормоконтролер : _____ / _____ /

КИІВ 2022

MINISTRY OF EDUCATION AND SCIENCE OF UKRAINE

NATIONAL AVIATION UNIVERSITY

**Aerospace Faculty
Aeroengines Department**

PERMISSION TO DEFEND

Head of department
Doctor of science, professor
Yu. Tereshchenko

“ _____ ” _____ 2022

MASTER’S DEGREE THESIS

Topic: *Measures to improve the fuel efficiency of power plants for
long-range passenger airplanes.*

Fulfilled by: Peng Xiaoxing

Supervisor:

Candidate of science (Engineering), assoc.prof. Gvozdetskyi I.I.

Labour precautions advisor:

Candidate of science (Engineering), assoc.prof Kazhan K. I.

Environmental protection advisor:

Candidate of science (Engineering), assoc.prof. Pavliukh L. I.

Standards Inspector _____ / _____ /

Kyiv 2022

НАЦІОНАЛЬНИЙ АВІАЦІЙНИЙ УНІВЕРСИТЕТ

Факультет Аерокосмічний факультет

Кафедра Авіаційних двигунів

Спеціальність 272 «Технічне обслуговування та ремонт ПС і авіадвигунів»

(шифр, найменування)

ЗАТВЕРДЖУЮ

Завідувач кафедри

Терещенко Ю.М.

“29” 09. 2022 р.

ЗАВДАННЯ

на виконання дипломної роботи

Пен Сяосін

(прізвище, ім'я, по батькові випускника в родовому відмінку)

- 1.Тема дипломної роботи: Заходи по підвищенню паливної ефективності силових установок на базі уніфікованого двоконтурного двигуна для дальньо-магістральних пасажирських літаків
затверджена наказом ректора від «29» 09. 2022 р. № 1786/ст
- 2.Термін виконання роботи : з 26 вересня 2022 р. по 30 листопада 2022р.
- 3.Вихідні дані до роботи (проекту): Розрахунки двигуна виконати для стартових умов ($H=0$, $V=0$, САУ), науково-дослідна частина: Дослідження методів і розробка заходів підвищення паливної ефективності авіаційних двоконтурних двигунів.
- 4.Зміст пояснювальної записки: Вступ, Аналіз сучасного стану і можливих способів покращення паливної ефективності літаків і силових установок, Вибір основних параметрів і газодинамічний розрахунок ТРДД, , розробка паливної системи, науково-дослідна частина, охорона праці, охорона навколишнього середовища, висновки по роботі.
- 5.Перелік обов'язкового графічного (ілюстративного) матеріалу: Конструктивно-силова схема двигуна і його паливної системи, графічні матеріали до науково- дослідної частини(схеми, графіки, діаграми).

6.Календарний план-графік

№ пор.	Завдання	Термін виконання	Відмітка про виконання
1	Огляд і аналіз літературних джерел по проблемі, розроблюваній у дипломній роботі	26.09.2022 05.10.2022	
2	Аналіз заходів по підвищенню паливної ефективності сучасних двоконтурних двигунів і розробка пропозицій по їх впровадженню.	06.10.2022 08.10.2022	
3	Вибір оптимальних параметрів робочого процесу та газодинамічний розрахунок двоконтурного двигуна за вибраними параметрами .	09.10.2022 16.10.2022	
4	Охорона праці	17.10.2022 20.10.2022	
5	Охорона навколишнього середовища	21.10.2022 24.10.2022	
6	Розробка паливної системи двигуна	25.10.2022 30.10.2022	
7	Розробка конструктивно-силової схеми двигуна	01.11. 2022 14.11.2022	
8	Розрахунки ефективності пропонованих заходів по підвищенню паливної ефективності силової установки	15.11.2022 16.11.2022	
9	Оформлення графічних матеріалів (конструктивної схеми двигуна і схеми паливної системи двигуна)	16.11.2022 18.11.2022	
10	Оформлення пояснювальної записки	18.11.2022 20.11.2022	

7.Консультанти з окремих розділів

Розділ	Консультант (посада, П.І.Б.)	Дата, підпис	
		Завдання видав	Завдання прийняв
Охорона навколишнього	<i>Павлюх Л.І.</i>		
Охорона праці	<i>Кажан К. І.</i>		

8.Дата видачі завдання: “ 10 ” 09 2022 р.

Керівник дипломної роботи _____ Гвоздецький І. І.
(підпис керівника) (П.І.Б.)

Завдання прийняв до виконання _____ Пен Сяосін
(підпис випускника) (П.І.Б.)

NATIONAL AVIATION UNIVERSITY

Faculty: The Aerospace faculty

Department: The Aeroengines Department

Educational and Qualifications level: Master's Degree

The specialty: 272 Technical Maintenance of Aircraft and Aeroengines

APPROVED BY

Head of the Department

Yu. Tereshchenko

“ ” 2022

Graduate Student's Degree Thesis Assignment

Name: Peng Xiaoxing

1. The Work (Thesis) topic: Measures to improve the fuel efficiency of power plants based on unified turbofan engines for long-range passenger airplanes.

Approved by the Rector's order of “ 29 ” 09 2022 № 1787/cm

2. The Graduation Project to be performed from : 26. 09. 2022 to 30. 11. 2022

3. Initial data for the project (thesis): TFE analyzed at standard atmospheric conditions (V=0; H=0; IST); The scientific research part: Measures of the fuel efficiency increase for the bypass engine; Projected turbofan engine designing and general conclusion

4. The content of the explanatory note (the list of problems to be considered: Introduction; Analysis of measures for aviation fuel consumption reducing; Projected turbofan engine designing; Labour precaution; Environment protection; Patent research; Contribution to fuel consumption with micro-circuit method of cooling; Analysis of engine functional systems; General conclusion

5. The list of mandatory graphic materials: Turbofan engine structural-load designed scheme; graphics and diagrams for scientific part of the diploma work

6. Time and Work Schedule

order #	Stages of Graduation Project Completion	Completion Dates	Remarks
1	Analytical part, review of factors impacting fuel consumption and measures related to fuel efficiency improvement	26.09.2022 05.10.2022	
2	Thermo-dynamic / Gas-dynamic calculation of gas turbine engine	06.10.2022 08.10.2022	
3	Gas-dynamic calculation of the axial turbine stage and Turbine rotor blade strength calculation	09.10.2022 16.10.2022	
4	Labour precaution	17.10.2022 20.10.2022	
5	Environment protection	21.10.2022 24.10.2022	
6	Evaluation of specific fuel consumption reduction due to micro-circuit method of cooling	25.10.2022 30.10.2022	
7	Development of structural- load scheme of engine	01.11. 2022 14.11.2022	
8	Calculations of efficiency of proposed measures for fuel consumptions of power plant reducing	15.11.2022 16.11.2022	
9	Arrangement of graphic materials (Structural –load scheme of engine and fuel supply system diagram)	16.11.2022 18.11.2022	
10	Arrangement of explanatory note	18.11.2022 20.11.2022	

7. Advisers on individual sections of the work (Thesis):

Section	Adviser	Date, Signature	
		Assignment Delivered	Assignment Accepted
Labour precaution	Kazhan K. I.		
Ecology	Pavliukh L. I.		

8. Assignment issue date: 29 . 09 . 2022

Graduate Project Supervisor: Gvozdetskyi I.I. _____
(supervisor signature)

Assignment is accepted for performing:

Graduate student : Peng Xiaoxing _____ 29 . 09 . 2022
(graduate student's signature) (Date)

CONTENTS

INTRODUCTION.....	10
Chapter 1 MAIN FACTORS INFLUENCE THE FUEL EFFICIENCY OF AIRCRAFT	
1.1 Influence parameters of engines.....	13
1.2 Influence of thermal efficiency.....	15
1.3 Influence of propulsive efficiency.....	17
1.3.1 Bypass ratio.....	18
1.3.2 Fan efficiency.....	21
Conclusion.....	23
Chapter 2 PROJECTED TURBOFAN ENGINE DESIGNING	
2.1 Gas-dynamic calculation of gas turbine engine.....	24
2.1.1 The fan inlet diameters calculations.....	25
2.1.2 Determination of parameters of fan stages.....	26
2.1.3 Compression work and number of high pressure turbine stages	
2.1.4 Parameters of the fan exit.....	27
2.1.5 Diameters of high-pressure compressor inlet.....	29
2.1.6 Diameters of high-pressure compressor exit.....	30
2.1.7 Diameters at high pressure turbine entrance.....	32
2.1.8 Diameters at the high-pressure turbine exit.....	33
2.1.9 Calculation the number of high-pressure compressor stages.....	35
2.1.10 Calculation the number of low-pressure compressor stages.....	36
2.1.11 Calculation of parameters at the low-pressure turbine entrance	

2.1.12 Calculation of diameters at the low-pressure turbine exit.....	37
2.1.13 Calculation of the turbofan engine jet nozzles.....	38
Chapter 3 Gas-dynamic Calculation Of The Axial Turbine Stage And Turbine Rotor Blade Strength Calculation	
3.1 Gas-dynamic Calculation of the axial turbine stage.....	41
3.2 Turbine rotor blade strength calculations.....	49
3.2.1 Tensile stresses in blade root caused by centrifugal forces.....	53
3.2.2 Bending stresses caused by gas forces.....	54
Conclusion.....	55
Chapter 4 LABOR PROTECTION	
4.1 Introduction.....	56
4.2 Harmful and hazardous working factors.....	56
4.3 Analysis of working conditions and development of protective measures.....	58
4.4 Fire Safety Rules at the workspace.....	59
4.5 Special requirement for precaution during maintenance of engine...	61
4.6 Occupational Safety and Health Protections.....	62
4.6.1 Face protection.....	62
4.6.2 Head protection.....	62
4.6.3 Respiratory protection.....	63
4.6.4 Body protection.....	63
Conclusion.....	64

Chapter 5	ENVIRONMENT PROTECTION	
5.1	Introduction.....	65
5.2	The emissions of greenhouse gases in aviation.....	66
5.3	Water pollution in aviation.....	69
5.4	Acoustic (noise) pollution.....	71
5.5	Soil contamination.....	73
5.6	Calculation of CO and NOx emissions by aircraft.....	77
5.7	Biofuels.....	80
	Conclusion.....	80
Chapter 6	FUEL CONSUMPTION REDUCTION WITH MICRO-CIRCUIT METHOD	
6.1	Quantitative analysis of the influence of g_{cool} on C_{sp}	83
6.2	Main specific parameters and mass flow rate calculation.....	87
	Conclusion.....	88
Chapter 7	ANALYSIS OF ENGINE FUEL SYSTEM	
7.1	Fuel delivery system.....	89
7.2	Automatic fuel control system.....	91
	GENERAL CONCLUSIONS.....	93
	REFERENCES.....	95

INTRODUCTION

Explanatory note on diploma work “Measures to improve the fuel efficiency of power plants based on unified turbofan engines for long-range passenger airplanes”. Unified turbofan engine based on prototype CFM-56-7B.

Introduction; Analysis of measures for aviation fuel consumption reducing; Projected turbofan engine designing; Labour precaution; Environment protection; Contribution to fuel consumption with micro-circuit method of cooling; Analysis of engine functional systems; General conclusion.

Airplane is an indispensable way of travel in our daily life, which greatly shortens our transportation time. In the case of the aircraft itself, fuel efficiency has always been a concern for designers and airlines. Analyzing the fuel efficiency of the air transport industry and its influencing factors has important practical significance for the air transport industry to achieve green and low-carbon development and reduce aviation carbon emissions and fuel costs.

So the topic of my paper is: Measures to improve the fuel efficiency of power plants based on unified turbofan engine.

In this diploma work, my goal is to improve fuel consumption efficiency, the main improvement methods are as follows:

- improve the parameters of working process
- improve the construction of the engine
- analyze and optimize the design parameters of the engine

Economics improve when airlines use unified engine airplanes. Because the unified engine will make the number of manufactures more, reduce the manufacturing cost and at the same time, the investment of the airlines on engine maintenance will also be reduced. Thus ensuring the benefits.

Many of the conclusions in this diploma project are based on the references of scientific research by examining relevant materials and also my own understanding and calculations. Of course, more professional analysis and improvement work still needs more experiments.

Chapter 1 MAIN FACTORS INFLUENCE THE FUEL EFFICIENCY OF AIRCRAFT

The ideas of improving aircraft fuel efficiency are mainly divided into the following aspects : materials 、 aerodynamics improvement、 aircraft systems、 engine improvement and so on.

Materials for airplane, especially the composite materials, are important. It can reduce the design weight of the aircraft, that means the aircraft will also have less take-off weight, and will need less thrust.

Aerodynamic improvements allow for reduced aerodynamic drag, which means that less engine thrust is required, resulting in lower fuel consumption.

Systems of aircraft (hydraulic、 electrical、 fuel、 pneumatic etc.) improving the efficiency of all functional systems can also lead to less needed thrust.

The improvement of engine performance can be divided into three categories:

- Improvement of parameters in the working process;
- Increase the efficiency of engine elements;
- Improved fuel property performance.

Each of these three ways will be discussed and explained further. All these measures will be introduced in follow-up studies.

Mainly, in this diploma section, I focus on the optimization of engine design, thus improving the engine performance to reduce specific fuel consumption.

1.1 Influence parameters of engines

Areas of action for improving engine fuel efficiency include the following :

- Air drag reduction;
- Reduced engine weight and size;
- Improves overall efficiency (reduces specific fuel consumption).

Engine drag is determined primarily by the size of the intake area (fan diameter) and nacelle surface (airflow range), and by the aerodynamic interaction between the nacelle and pylon, and between the pylon and wing. The drag of the mounted engine is due to this. Engine weight mainly depends on factors such as engine size (fan diameter), number of components, design and materials.

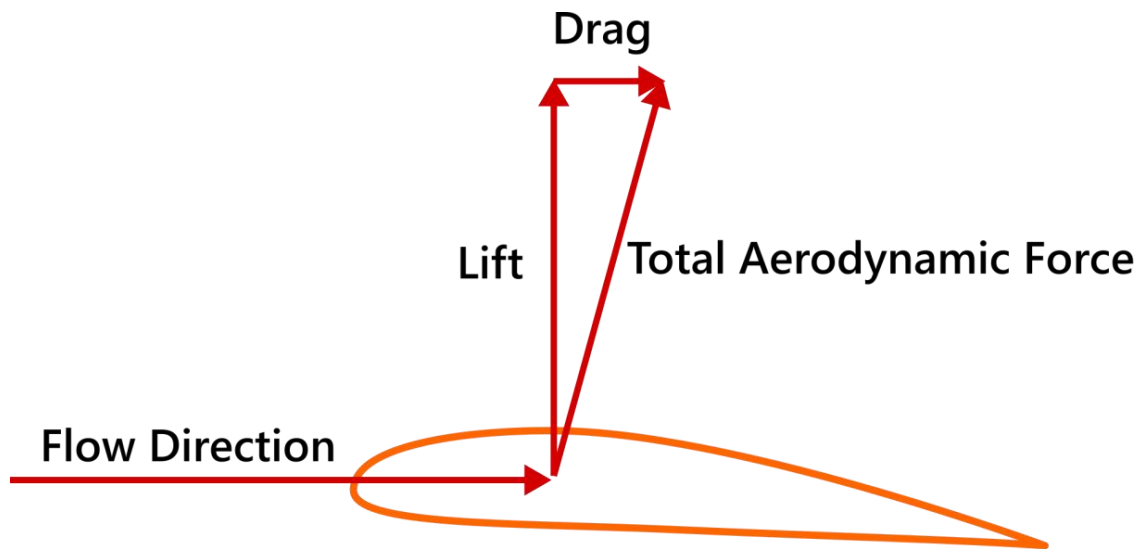


Fig1.1.Lift and drag , two components of the total aerodynamic force acting on an aerofoil

Specific fuel consumption is the amount of fuel consumed by a vehicle for each unit of power output. The specific fuel consumption of an engine is the rate of fuel burnt to produce a unit of thrust. The definition of specific fuel consumption describes the ratio of fuel consumed to thrust produced, and an engine's specific fuel consumption is primarily determined by engine cycle data. The most important thermodynamic cycle parameters affecting specific fuel consumption are:

- Overall Pressure Ratio ;
- Turbine inlet temperature ;
- Bypass Ratio.

The overall efficiency of an engine system is expressed as the product of thermal efficiency and propulsive efficiency.

For a heat engine, thermal efficiency is the ratio of the net work output to the heat input. Thermal efficiency describes only the mass of chemicals within the engine components that are converted to kinetic energy, whereas overall efficiency is defined as the ratio of the energy converted to thrust and the energy provided by the core engine. Propulsive efficiency is also taken into account. The fuel consumption rate can be reduced by improving propulsive and thermal efficiency. It can also be reduced by using alternative fuels with higher specific calorific values (e.g. hydrogen) and lower flight speeds.

1.2 Influence of thermal efficiency

The thermal efficiency of an aircraft engine is the ratio of energy output to energy input. This also determines the specific core engine performance. Thermal efficiency represents the mass of the engine as a thermal device and expresses the ratio of power output to heat flow input. It is an indicator of the quality of the thermodynamic cycle through which thermal energy is converted into thrust. Figure 1.2 shows the dependence of thermal efficiency on turbine inlet temperature[1] ; Figure 1.3 shows the dependence of thermal efficiency and overall pressure ratio[2].

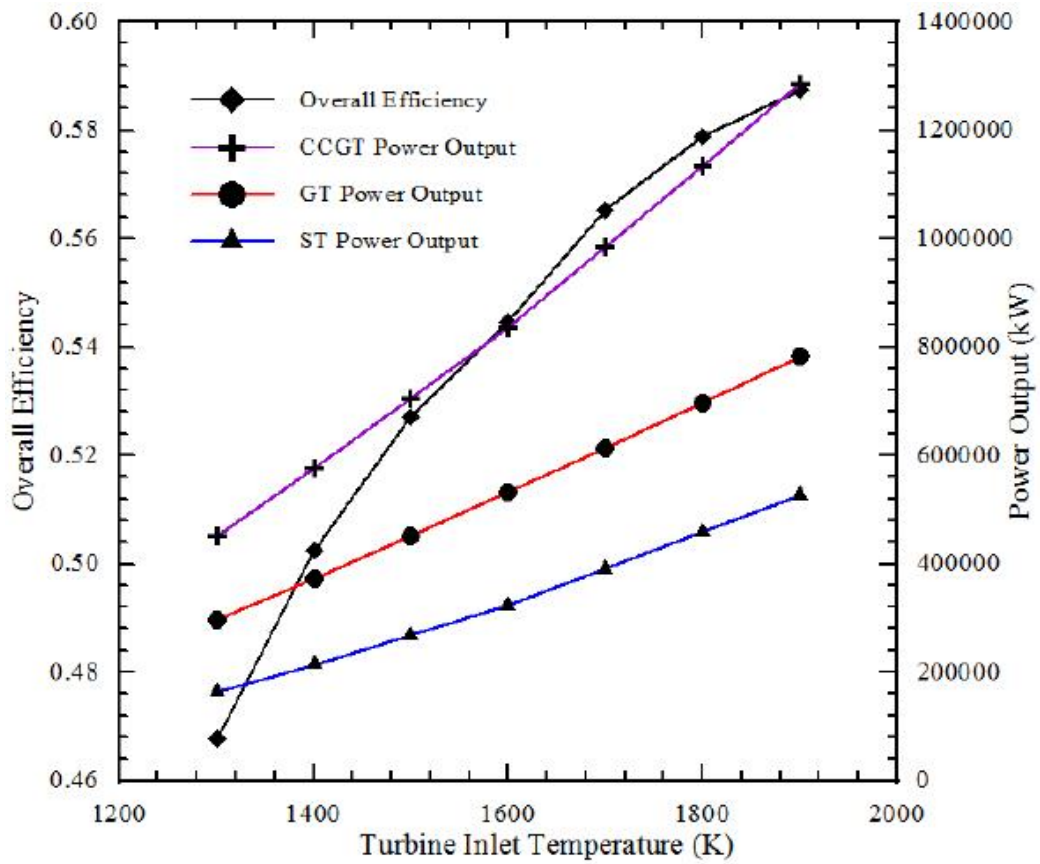


Fig1.2 Effect of Turbine inlet temperature on the overall performance

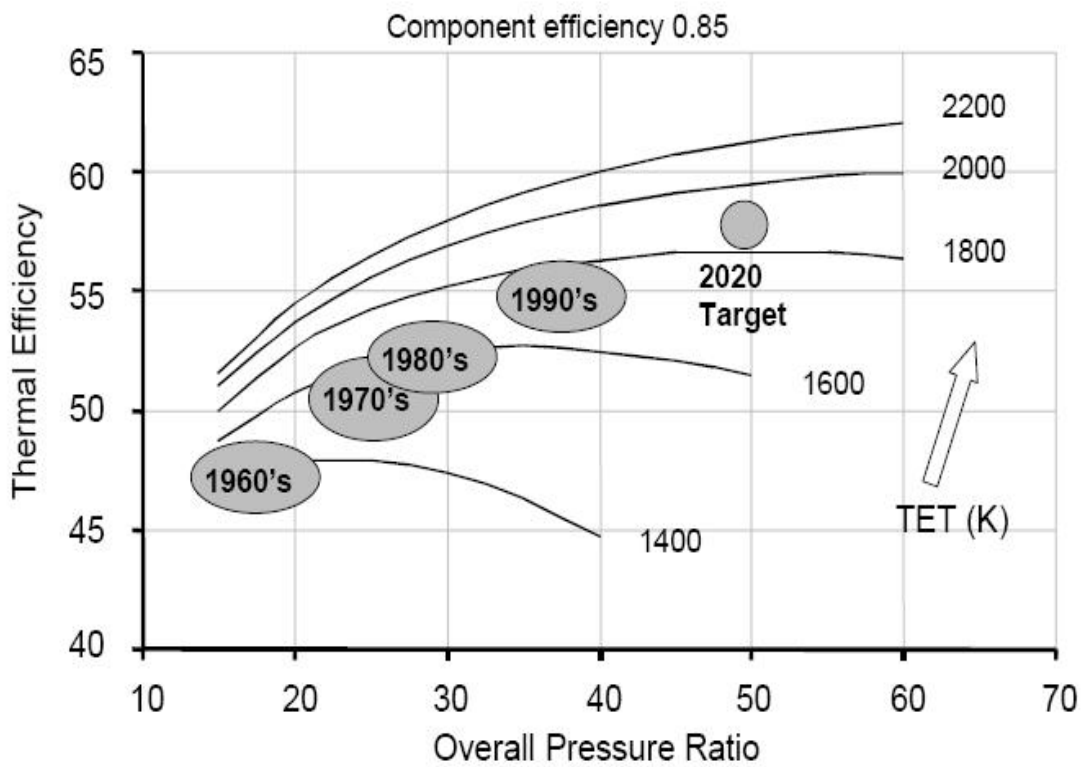


Fig.1.3 Thermal efficiency dependent on Overall Pressure Ratio

As can be seen from the above figures , Efficiency can be increased by increasing component efficiency (increased efficiency of compressors, turbines, combustors, fuel lines, etc.) or by modifying cycle parameters (higher turbine inlet temperature and overall pressure ratio).

1.3 Influence of propulsive efficiency

The efficiency of a propulsor-propulsive efficiency η_p , is the portion of the available energy that is usefully applied in propelling the aircraft compared to the total energy of the jet stream. It expresses the ratio of the energy converted into thrust to the energy available to the core engine for propulsion. These include fan propulsion efficiency, low pressure (LP) system component efficiency, core engine jet efficiency, and gear and jet nozzle or nacelle drag losses. It initially depends on the ratio of exhaust gas velocity to airspeed and increases as the ratio decreases. Accordingly, the propulsive efficiency can be improved by reducing the nozzle ejection speed.

In order to continuously generate thrust, the airflow must be increased accordingly, for example by increasing the inlet diameter. This means that the specific thrust is reduced. With a constant demand for thrust, this will lead to a further increase in the bypass ratio in the future, which leads to an enlarged inlet diameter. These measures ca

n only be successfully implemented by reducing the air resistance in the nacelle and increasing the efficiency of the fans[3].

1.3.1 Bypass ratio

The bypass ratio (BPR) of a turbofan engine is the ratio between the mass flow rate of the bypass stream to the mass flow rate entering the core. A 10:1 bypass ratio, for example, means that 10 kg of air passes through the bypass duct for every 1 kg of air passing through the core[4].

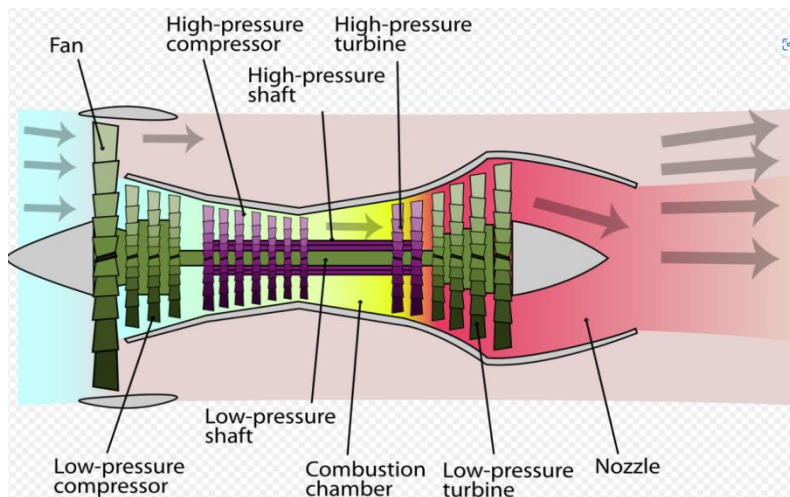


Fig 1.4 high-bypass engine

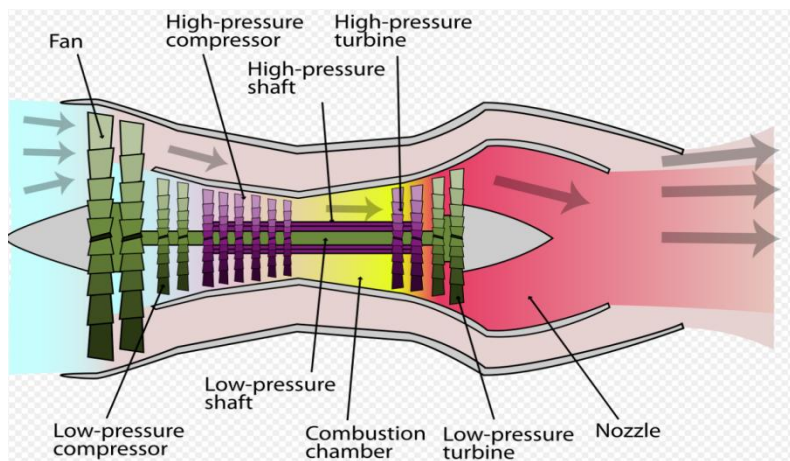


Fig 1.5 low-bypass engine

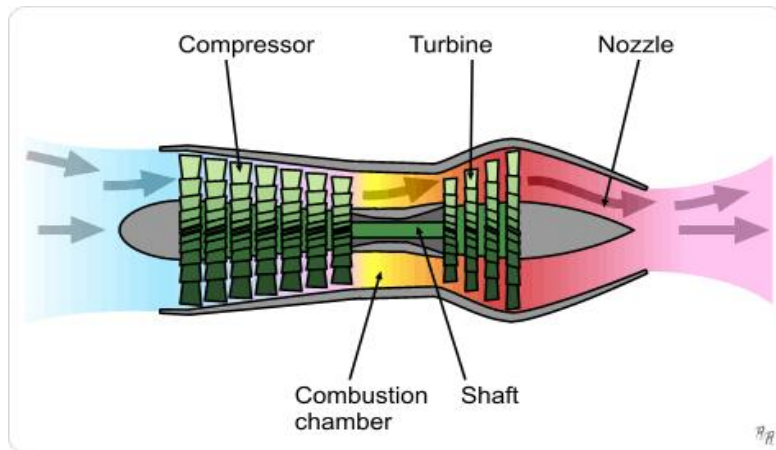


Fig 1.6 turbojet engine

The high-bypass engine (top) has a large fan that routes much air around the turbine; the low-bypass engine (middle) has a smaller fan routing more air into the turbine; the turbojet (bottom) has zero bypass, and all air goes through the turbine.

Above a certain BPR, the increased weight and drag offset the positive effects of increased propulsion efficiency. In addition, engine thrust decreases with increasing flight altitude and decreasing atmospheric density at high bypass ratios. Because at a constant fan speed, the mass flow in the area outside the engine is reduced. More fuel must be provided in the air to provide the same thrust as on the ground. This effect actually counteracts the reduced drag at altitude by reducing the density of the atmosphere.

The use of new designs as well as improved materials and new technologies can translate this optimization into lower fuel consumption and higher bypass ratio.

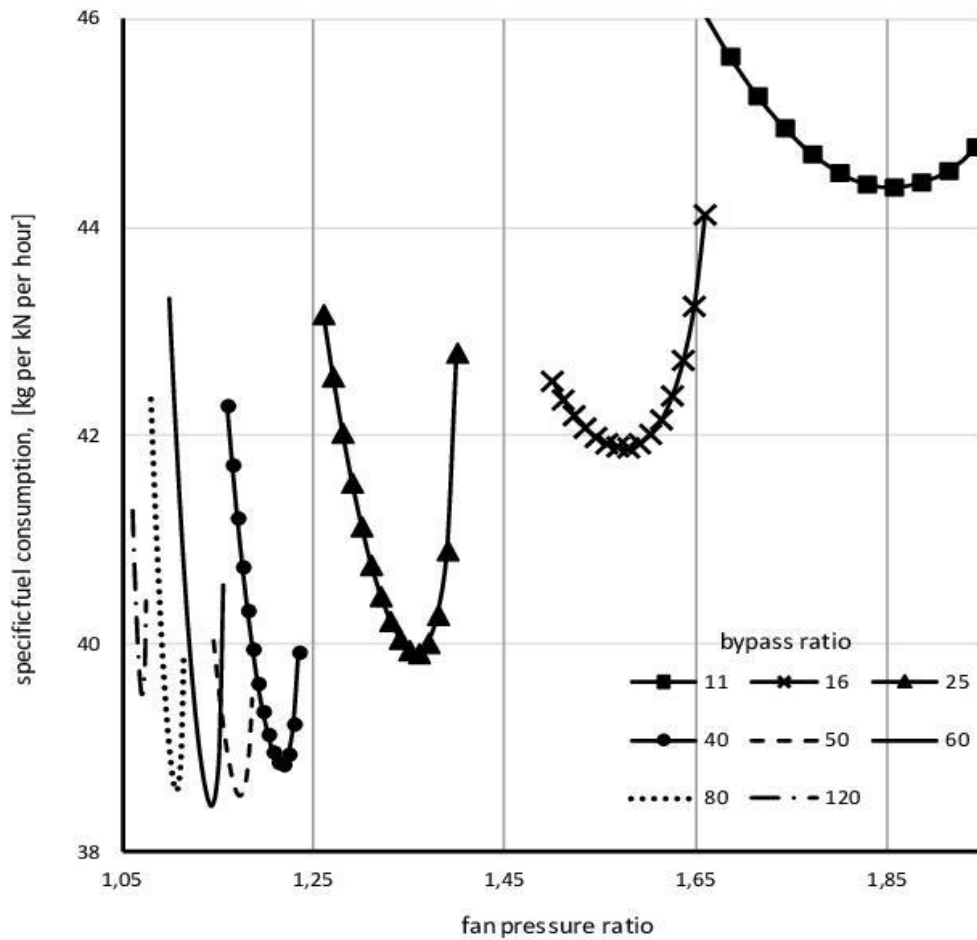


Fig1.7 Specific fuel consumption against the bypass ratio[5].

Figure 1.8 shows propulsion thrust as a function of specific thrust, fan intake Mach number, and fan pressure ratio for a given thrust. As the diameter of the fan increases, the specific thrust decreases and the propulsion efficiency increases, thereby reducing the specific fuel consumption[6].

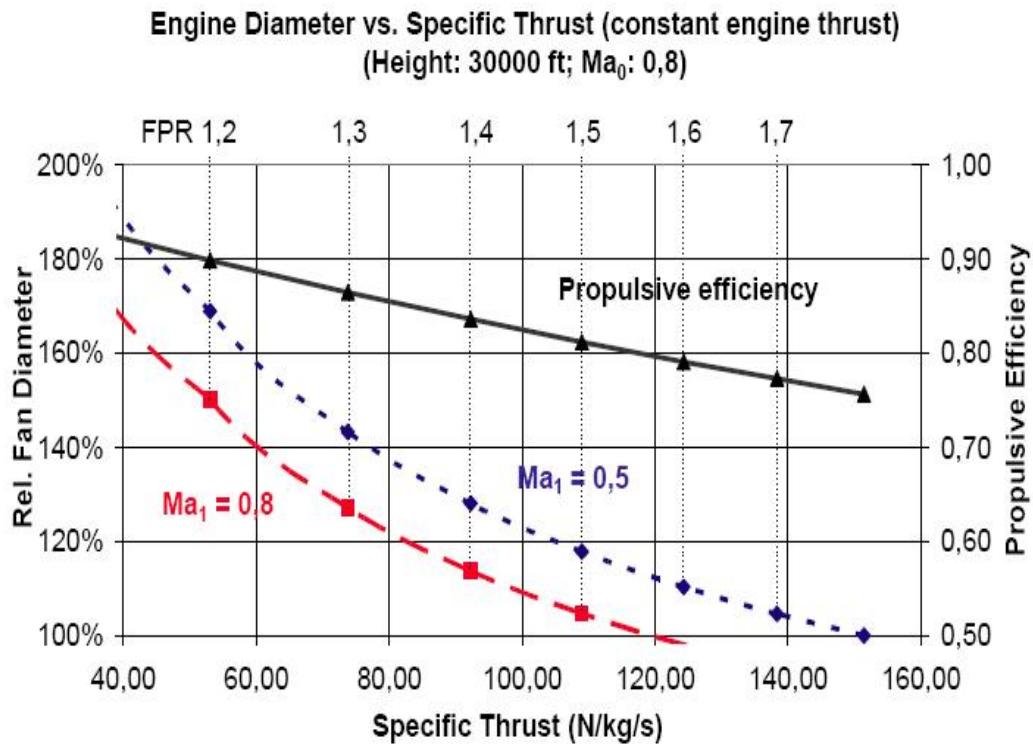


Fig.1.8 Propulsive efficiency and fan diameter depending on specific thrust

As shown in Figure 1.8, the fan pressure ratio is an important parameter to improve propulsion efficiency. As the fan pressure ratio increases, the propulsion efficiency increases.

1.3.2 Fan efficiency

The lower the ratio of jet speed to flight speed, the higher the fan efficiency (propeller efficiency). In particular, for a given thrust, choose a large fan diameter and bypass ratio and a small fan pressure ratio.

The large bypass ratio and the small fan pressure ratio lead to a lower specific thrust and thus to a lower specific fuel consumption. For each fan pressure ratio there is a minimum SFC, which has to be adjusted to the corresponding thermodynamic cycle by the size of the bypass and a certain thrust. The reason for this is the changed nozzle pressure ratio, which affects the optimum specific thrust. If the FPR is too small, too much radiant heat energy is wasted because too little energy is extracted from the core flow. If the blower pressure ratio is too high, energy is lost due to the high jet velocity in the bypass duct.

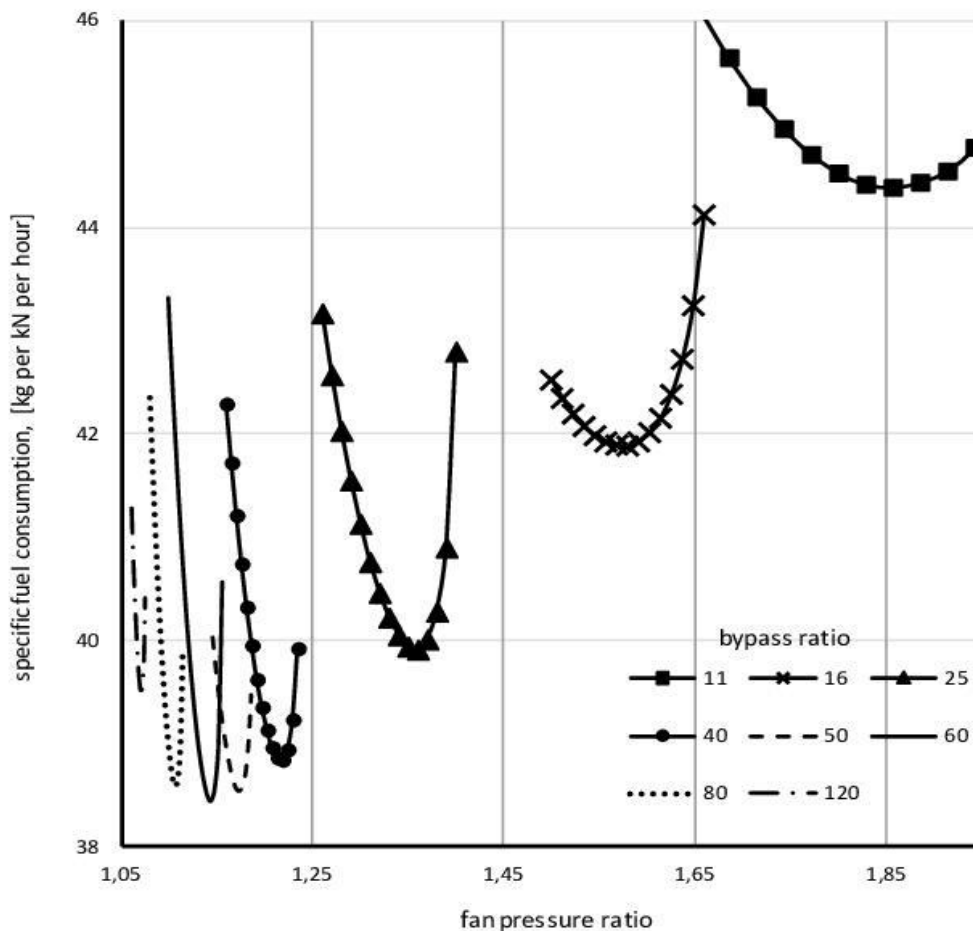


Fig.9.9 Specific fuel consumption against fan pressure ratio[5].

Conclusion:

In this chapter, many feasible measures have been analyzed, from the results we know how to reduce specific fuel consumption. Such as increasing the turbine inlet diameter 、 increasing diameter of the fan、 higher bypass ratio and so on.

Chapter 2 PROJECTED TURBOFAN ENGINE DESIGNING

2.1 Gas-dynamic calculation of gas turbine engine

Gas-dynamic calculation is performed in accordance with method guide[7].TFE analyzed at standard atmospheric conditions (V=0; H=0; I ST).

Table 2.1

Parameter	Designation	Unit	Value
Thrust	R	kN	120
Fan Pressure ratio	π_{fan}^*	-	1.6
Pressure ratio in the compressor	π_c^*	-	30
Bypass ratio	m	-	5
Gas temperature in the combustion chamber outlet	T_g^*	K	1500
Pressure on an inlet	P_H	Pa	101325
Temperature on an inlet	T_H	K	288

Engine type – Turbofan engine;

Thrust: $P=120000$ N;

Mass flow rate: $G=374.4$ kg/s;

Bypass ratio: $m=5$;

Compressor pressure ratio: $\pi_c^* = 30$;

Fan pressure ratio: $\pi_f^* = 1.6$;

Temperature of a gas entering turbine: $T_g^* = 1500K$;

2.1.1 The fan inlet diameters calculations

Mass flow rate: $G=374.4$ kg/s

in order to reduce the engine diametrical sizes we set:

axial air speed: $c_{1a} = 210$ m/s

fan tip circumferential velocity: $u_{1ft} = 490$ m/s

relative diameter of the first stage fan sleeve: $d_1 = 0.3$

air flow reduced velocity λ_{1a} :

$$\lambda_{1a} = \frac{c_{1a}}{c_{1cr}} = \frac{c_{1a}}{18.3 \sqrt{T_{fi}^*}} = \frac{210}{18.3 \cdot \sqrt{288}} = 0.6762$$

Relative density of air flows:

$$q(\lambda_{1a}) = \frac{G}{G_{max}} = \frac{c\rho}{c_{cr}\rho_{cr}} = \left(\frac{k+1}{2}\right)^{\frac{1}{k-1}} \lambda_{1a} \left(1 - \frac{k-1}{k+1} \lambda_{1a}^2\right)^{\frac{1}{k-1}}$$

Where $k=1.4$, then we can calculate $q(\lambda_{1a}) = 0.875$

The fan (or compressor) inlet area:

$$F_{fi} = \frac{G_a \sqrt{T_{fi}^*}}{m_a p_{fi}^* q(\lambda_{1a})} = \frac{374.4 \cdot \sqrt{288}}{0.040348 \cdot 1 \cdot 10^5 \cdot 0.875} = 1.799 \text{ m}^2$$

Where $m_a = 0.040348$

the first-stage sleeve relative diameter $\bar{d}_1 = \frac{D_{1sl}}{D_{1ft}} = 0.3$ is to be selected in

accordance with recommendation.

The fan external diameter at the inlet in the first stage:

$$D_{1ft} = \sqrt{\frac{4F_{fi}}{\pi(1-\bar{d}_1^2)}} = \sqrt{\frac{4 \cdot 1.799}{3.14 \cdot (1-0.3^2)}} = 1.585 \text{ m}$$

Approximate to $D_{1ft} = 1.59$ m

sleeve diameter:

$$D_{1sl} = \sqrt{D_{1ft}^2 - \frac{4F_{fi}}{\pi}} = \sqrt{1.59^2 - \frac{4}{3.14} \cdot 1.799} = 0.459 \text{ m}$$

Diameter of conditional section separating the primary and secondary air

flows:

$$\begin{aligned} D_1 &= \sqrt{D_{1ft}^2 - \frac{4F_{II}}{\pi}} = \sqrt{D_{1ft}^2 - \frac{4}{\pi} \frac{G_{aII}}{G_a} F_{fi}} \\ &= \sqrt{1.59^2 - \frac{4}{3.14} \cdot \frac{312}{374.4} \cdot 1.799} = 0.602 \text{ m} \end{aligned}$$

Where $G_a = 374.4$ kg/s, $G_{aII} = 312$ kg/s

2.1.2 Determination of parameters of fan stages

Blade circumferential velocity at the diameter D_1 :

$$u_1 = u_{1ft} \cdot \frac{D_1}{D_{1ft}} = 490 \cdot \frac{0.602}{1.585} = 186.1 \text{ m/s}$$

The lattice density near the sleeve is assumed as $\left(\frac{b}{t}\right)_{sl} = 2.2$

the lattice density, air twisting in rotor blades and work imparted to the air

by the fan blades on the diameter D_1 :

$$\begin{aligned} \left(\frac{b}{t}\right)_1 &= \left(\frac{b}{t}\right)_{sl} \cdot \frac{D_{1sl}}{D_1} = 2.2 \cdot \frac{0.459}{0.602} = 1.677 \\ \Delta W_{u_1} &\cong c_{1a} \cdot \frac{1.55}{1 + 1.5 \cdot \left(\frac{t}{b}\right)_I} \approx 210 \cdot \frac{1.55}{1 + 1.5 \cdot \frac{1}{2.2}} = 193.5 \text{ m/s} \end{aligned}$$

$$L_1 = u_1 \cdot \Delta W_{u_1} = 193.5 \cdot 186.1 = 36 \frac{kJ}{kg}$$

Finally we get:

$$D_{1_{ft}} = 1.59 \text{ m}; D_I = 0.602 \text{ m}; u_{1_{ft}} = 490 \text{ m/s}; L_{fan_I} = 36 \frac{kJ}{kg}$$

2.1.3 Compression work and number of high pressure turbine stages

the work of high-pressure compressor:

$$L_{hpc} = L_c - L_{fan_I} - L_{lpc} = 581 - 36.0 - 48.0 = 497.0 \frac{kJ}{kg}$$

the work of high-pressure turbine:

$$L_{hpt} = \frac{L_{hpc}}{(1 + g_f)(1 - g_{cool})\eta_m} = \frac{497.0}{(1 + 0.0207) \cdot (1 - 0.03) \cdot 0.99}$$

$$= 507.1 \frac{kJ}{kg}$$

$$g_{cool} = 0.03; \text{ set } Y^* = 0.35; z=1, \eta_t^* = 0.91$$

circumferential velocity on middle turbine radius:

$$u_{t_{md}} = Y^* \sqrt{\frac{2L_{hpt}}{z\eta_{hpt}}} = 0.35 \cdot \sqrt{\frac{2 \cdot 507100}{1 \cdot 0.91}} = 369.5 < 400 \text{ m/s}$$

Finally we get a two-stage scheme of the engine and select a single-stage

high pressure turbine and one-stage fan with added compressor stages.

$$L_{st_1} = 507 \frac{kJ}{kg} \quad L_{fan_I} = 36.0 \frac{kJ}{kg} \quad L_{lpc} = 48.0 \frac{kJ}{kg}$$

2.1.4 Parameters of the fan exit

$$\text{Assuming } \eta_{lpc}^* = \eta_{fan_{II}}^* = 0.91$$

pressure ratio in low-pressure compressor:

$$\pi_{lpc}^* = \left(1 + \frac{L_{lpc} \eta_{lpc}^*}{\frac{k}{k-1} RT_{fi}^*} \right)^{\frac{k}{k-1}} = \left(1 + \frac{36000 \cdot 0.91}{3.5 \cdot 287 \cdot 288} \right)^{\frac{1.4}{1.4-1}} = 1.46$$

total air temperature:

$$T_{lpcd}^* = T_{fi}^* + \frac{k-1}{k} \cdot \frac{L_{lpc}}{R} = 288 + 0.286 \cdot \frac{36000}{287} = 323.87 \text{ K}$$

total air pressure:

$$P_{lpcd}^* = P_{fi}^* \pi_{lpc}^* = 1 \cdot 10^5 \cdot 1.6 = 1.6 \cdot 10^5 \text{ Pa}$$

pressure ratio of booster $\pi_{lpc} = 1.15^3 = 1.52$; $\eta_{lpc}^* = 0.89$

$$\begin{aligned} L_{lpc} &= \frac{k}{k-1} RT_{fdII}^* \left(\pi_{lpc}^{\frac{k-1}{k}} - 1 \right) \frac{1}{\eta_{lpc}^*} \\ &= \frac{1.4}{1.4-1} \cdot 287 \cdot 333.5 \cdot (1.52^{0.286} - 1) \cdot \frac{1}{0.89} = 48.0 \frac{\text{kJ}}{\text{kg}} \end{aligned}$$

The total air pressure:

$$p_{lpc}^* = p_{fdII}^* \cdot \pi_{lpc} = 1.6 \cdot 10^5 \cdot 1.52 = 2.43 \cdot 10^5 \text{ Pa}$$

For turbofan engine with a fan with added compressor stages:

$$\lambda_{a_{fanI}} = \frac{c_{a_{fanI}}}{c_{cr}} = \frac{c_{a_{fanI}}}{18.3 \cdot \sqrt{T_{fdI}^*}} = \frac{200}{18.3 \cdot \sqrt{323.87}} = 0.607$$

$$\lambda_{a_{fanII}} = \frac{c_{a_{fanII}}}{c_{cr}} = \frac{c_{a_{fanII}}}{18.3 \cdot \sqrt{T_{fdII}^*}} = \frac{200}{18.3 \cdot \sqrt{333.5}} = 0.598$$

$$q(\lambda_{a_{fanI}}) = 1.5774 \lambda_{a_{fanI}} \left(1 - \frac{1}{6} \lambda_{a_{fanI}}^2 \right)^{2.5} = 0.817$$

$$q(\lambda_{a_{fanII}}) = 1.5774 \lambda_{a_{fanII}} \left(1 - \frac{1}{6} \lambda_{a_{fanII}}^2 \right)^{2.5} = 0.808$$

$$F_{fan_I} = \frac{G_{a_I} \sqrt{T_{fd_I}^*}}{m_a p_{fd_I}^* q(\lambda_{a_{fan_I}})} = \frac{62.4 \cdot \sqrt{323.87}}{0.040348 \cdot 1.6 \cdot 10^5 \cdot 0.817} = 0.213 \text{ m}^2$$

$$F_{fan_{II}} = \frac{G_{a_{II}} \sqrt{T_{fd_{II}}^*}}{m_a p_{fd_{II}}^* q(\lambda_{a_{fan_{II}}})} = \frac{312 \cdot \sqrt{333.48}}{0.040348 \cdot 1.6 \cdot 10^5 \cdot 0.808} = 1.032 \text{ m}^2$$

external diameter behind the fan:

$$D_{fan_{II}} = 0.95 \cdot D_{1_{ft}} = 0.95 \cdot 1.59 = 1.51 \text{ m}$$

The diameter of the section dividing the primary and secondary air flows:

$$D_{II} = \sqrt{D_{fan_{II}}^2 - \frac{4}{\pi} \cdot F_{fan_{II}}} = \sqrt{1.51^2 - \frac{4}{3.14} \cdot 1.032} = 0.9333 \text{ m}$$

$$D_{II} = 0.9333 - 0.020 = 0.913 \text{ m (separating ring thick 20mm)}$$

Sleeve diameter:

$$D_{fan_{sl}} = \sqrt{D_{II}^2 - \frac{4}{\pi} F_{fan_I}} = \sqrt{0.913^2 - \frac{4}{3.14} \cdot 0.213} = 0.755 \text{ m}$$

Finally we get:

$$\text{The primary flow - } D_{fan_{sl}} = 0.755 \text{ m, } D_{fan_I} = 0.913 \text{ m}$$

$$\text{The secondary flow - } D_{fan_{II}} = 1.510 \text{ m, } D_{II} = 0.933 \text{ m}$$

2.1.5 Diameters of high-pressure compressor inlet

$$\text{Air temperature: } T_{a_{hpc}}^* = T_{fan_I}^* = 323.87 \text{ K}$$

Air pressure taking into account losses:

$$P_{a_{hpc}}^* = P_{fan_I}^* \sigma = 2.43 \cdot 10^5 \cdot 0.98 = 2.38 \cdot 10^5 \text{ Pa}$$

set air speed at the inlet to the high-pressure compressor:

$$C_{a_{hpc}} = 195 \text{ m/s}$$

$$\lambda_{a_{hpc}} = \frac{C_{a_{hpc}}}{18.3 \sqrt{T_{fanI}^*}}$$

$$= \frac{195}{18.3 \cdot \sqrt{323.87}} = 0.532$$

$$q(\lambda)_{a_{hpc}} = 0.792$$

$$F_{a_{hpc}} = \frac{G_{aI} \sqrt{T_{fanI}^*}}{m_a p_{a_{hpc}}^* q(\lambda_{a_{hpc}})}$$

$$= \frac{62.4 \cdot \sqrt{323.87}}{0.040348 \cdot 1.49 \cdot 10^5 \cdot 0.792} = 0.23 \text{ m}^2$$

Relative diameter of the working wheel at at the high-pressure compressor inlet $d_b = 0.5\text{m}$

$$\text{external diameter } D_{I_{hpc}} = \sqrt{\frac{4F_{a_{hpc}}}{\pi(1-d_b^2)}} = \sqrt{\frac{4 \cdot 0.23}{3.14 \cdot (1-0.5^2)}} = 0.62 \text{ m}$$

The first stage working wheel sleeve diameter of a high-pressure compressor:

$$D_{sl_{hpc}} = \sqrt{D_{I_{hpc}}^2 - \frac{4}{\pi} \cdot F_{a_{hpc}}}$$

$$= \sqrt{0.62^2 - \frac{4}{3.14} \cdot 0.23} = 0.455 \text{ m}$$

The height of the working wheel blade:

$$h_b = \frac{D_{I_{hpc}} - D_{sl_{hpc}}}{2}$$

$$= \frac{0.62 - 0.455}{2} = 0.0825 \text{ m}$$

2.1.6 Diameters of high-pressure compressor exit

Air temperature behind the high-pressure compressor:

$$T_c^* = T_{hpc}^* + \frac{L_{hpc}}{\frac{k}{k-1}R}$$

$$= 323.87 + \frac{497000}{\frac{1.4}{1.4-1} \cdot 288} = 815.9 \text{ K}$$

The pressure ratio in high-pressure compressor:

$$\pi_{hpc}^* = \frac{P_c^*}{P_{a_{hpc}}^*} = \frac{32}{2.38} = 13.4$$

Assuming the airspeed at the exit of high-pressure compressor is 110 m/s

$$\lambda = \frac{C}{18.3\sqrt{T^*}} = \frac{110}{18.3 \cdot \sqrt{816}} = 0.2104$$

$$q(\lambda) = 0.31$$

The cross-section area at the high-pressure compressor exit:

$$F_c = \frac{G_{aI}\sqrt{T_c^*}}{m_a p_{a_{hpc}}^* q(\lambda_{a_c})}$$

$$= \frac{62.4 \cdot \sqrt{816}}{0.040348 \cdot 32 \cdot 10^5 \cdot 0.31} = 0.0445 \text{ m}^2$$

$$D_{sl.c} = \sqrt{D_{I_{hpc}}^2 - \frac{4}{\pi} F_c} = \sqrt{0.62^2 - \frac{4}{3.14} \cdot 0.0445} = 0.57 \text{ m}$$

$$h_b = \frac{D_{I_{hpc}} - D_{sl.c}}{2} = \frac{0.62 - 0.57}{2} = 0.025 \text{ m}$$

$$d_{sl.c} = \frac{D_{sl.c}}{D_{I_{hpc}}} = \frac{0.57}{0.62} = 0.919 \text{ m}$$

To reduce the value of $d_{sl.c}$ at the high-pressure compressor exit we must decrease diameter D_c of the last stage to 0.6m.

$$D_{sl.c} = \sqrt{0.6^2 - \frac{4}{3.14} \cdot 0.0445} = 0.55 \text{ m}$$

$$h_b = \frac{0.6 - 0.5507}{2} = 0.0246 \text{ m}$$

$$d_{sl.c} = \frac{0.55}{0.6} = 0.916 \text{ m}$$

Finally we get:

at the high-pressure compressor entrance $D_c = 0.62 \text{ m}$, $D_{sl} = 0.455 \text{ m}$,

$h_b = 82.5 \text{ mm}$

at the high-pressure compressor exit $D_c = 0.6 \text{ m}$, $D_{sl} = 0.550 \text{ m}$, $h_b =$

24.6 mm

2.1.7 Diameters at high pressure turbine entrance

$$U_{c mn} = 413 \text{ m/s}$$

assumed work for the first stage $L_{st_1} = 270 \frac{\text{kJ}}{\text{kg}}$, We set the angle of a

stream outlet from nozzle diaphragm $\alpha_1 = 20^\circ$

jet velocity of gas emission from the ND:

$$C_1 = \frac{L_{st_1}}{u_{t mn} \cos \alpha_1} = \frac{270000}{413 \cdot 0.9397} = 696 \text{ m/s}$$

$$\lambda_1 = \frac{C_1}{C_{cr}} = \frac{696}{18.15 \cdot \sqrt{1500}} = 0.974$$

$$q(\lambda_{1ca}) = 0.999$$

The gas flow rate G_g :

$$G_G = G_{a_1} (1 + g_f) (1 - g_{cool})$$

$$G_G = 62.4 \cdot (1 + 0.0207) \cdot (1 - 0.05) = 60.5 \text{ kg/s}$$

The gas pressure at the exit of the turbine nozzle diaphragm:

$$P_{nd}^* = P_{cd} \sigma_{cc} \sigma_{nd} = 32 \cdot 10^5 \cdot 0.98 \cdot 0.98 = 30.8 \cdot 10^5 \text{ Pa}$$

The cross section area at the nozzle diaphragm exit:

$$F_{I_{nd}} = \frac{G_g \sqrt{T_{ti}^*}}{m_g p_{nd}^* q(\lambda_{nd}) \sin \alpha_1}$$

$$= \frac{60.5 \cdot \sqrt{1500}}{0.0396 \cdot 30.8 \cdot 10^5 \cdot 0.999 \cdot 0.3420} = 0.056 \text{ m}^2$$

assume that $D_{tmd} = 0.685 \text{ m}$

the length of turbine blade:

$$h_b = \frac{F_{I_{nd}}}{\pi D_{tmd}} = \frac{0.056}{3.14 \cdot 0.685} = 0.0303 \text{ m}$$

$$D_t = D_{tmd} + h_b = 0.685 + 0.0303 = 0.715 \text{ m}$$

Set $D_t = 0.72 \text{ m}$

$$D_{sl} = \sqrt{D_t^2 - \frac{4}{\pi} F_{I_{nd}}} = \sqrt{0.72^2 - \frac{4}{3.14} \cdot 0.056} = 0.65 \text{ m}$$

at the turbine wheel of the high-pressure turbine inlet:

$$D_t = 0.72 \text{ m}; D_{sl} = 0.65 \text{ m}; D_{tmd} = 0.6 \text{ m};$$

$$h_b = \frac{0.72 - 0.65}{2} = 0.035 \text{ m}$$

The axial velocity of the gas at the turbine wheel entrance:

$$C_{1_a} = c_1 \sin \alpha_1 = 696 \cdot 0.3420 = 238 \text{ m/s}$$

2.1.8 Diameters at the high-pressure turbine exit

$$T_{hpt}^* = T_{ti}^* - \frac{L_{hpt}}{\frac{k_g}{k_g - 1} R_g} = 1500 - \frac{513000}{4 \cdot 288} = 1055 \text{ K}$$

$$p_{hpt}^* = p_{ti}^* \left(1 - \frac{T_{ti}^* - T_{hpt}^*}{T_{ti}^* \eta_{hpt}^*} \right)^{\frac{k_g}{k_g - 1}}$$

$$= 32 \cdot 10^5 \cdot 0.98 \cdot \left(1 - \frac{1500 - 1055}{1500 \cdot 0.91} \right)^4 = 6.9 \cdot 10^5 \text{ Pa}$$

We set the reduced gas velocity $\lambda_{2_a} = 0.55$

gas speed at the high-pressure turbine exit:

$$C_{2_a} = 0.55 \cdot 18.15 \cdot \sqrt{1055} = 324.24 \text{ m/s}$$

$$q(\lambda_{2_a}) = 1.5774 \cdot \lambda_{2_a} \left(1 - \frac{1}{6} \lambda_{2_a}^2 \right)^{2.5} = 0.7651$$

As some of the cooling air mixes with the airflow, we assume $g_{cool_2} =$

0.08, the gas flow rate at the high-pressure turbine exit:

$$G_G = G_{a_1} (1 + g_f) (1 - g_{cool_2})$$

$$G_G = 62.4 \cdot (1 + 0.0207) \cdot (1 - 0.08) = 61.15 \frac{\text{kg}}{\text{s}}$$

The cross-section area at the high-pressure turbine exit:

$$F_{hpt} = \frac{G_g \sqrt{T_{hptd}^*}}{m_g p_{hptd}^* q(\lambda_{2_a})}$$

$$F_{hpt} = \frac{61.15 \cdot \sqrt{1055}}{0.0396 \cdot 6.9 \cdot 10^5 \cdot 0.7651} = 0.095 \text{ m}^2$$

Assume $D_{tav} = 0.695 \text{ m}$

the height of the blade of the high-pressure turbine second stage:

$$h_b = \frac{F_{hpt}}{\pi D_{tav}} = \frac{0.095}{3.14 \cdot 0.695} = 0.044 \text{ m}$$

$$D_{hpt} = D_{tav} + h_b = 0.695 + 0.044 = 0.739 \text{ m}$$

Assume $D_{hpt} = 0.75$, HPT sleeve diameter $D_{sl_{hpt}}$:

$$D_{sl_{hptd}} = \sqrt{D_{hptd}^2 - \frac{4}{\pi} F_{hptd}}$$

$$D_{sl_{hptd}} = \sqrt{0.750^2 - \frac{4}{3.14} \cdot 0.095} = 0.664m$$

2.1.9 Calculation the number of high-pressure compressor stages

The work of the HPC first stage is calculated assuming that the lattice

density is $\left(\frac{b}{t}\right)_{sl} = 2.5$

$$c_{1a} = 180m/s$$

$$\Delta W_{u_{sl}} = c_{1a} \frac{1.55}{1 + 1.5 \frac{t}{b}} = 180 \cdot \frac{1.55}{1 + 1.5 \frac{1}{2.5}} = 174.4 m/s$$

$$u_{1_{sl}} = u_{t_{md}} \frac{D_{1_{sl}}}{D_{t_{md}}} = 413 \cdot \frac{0.455}{0.58} = 324 m/s$$

$$u_{1_c} = u_{t_{av}} \frac{D_c}{D_{t_{av}}} = 413 \cdot \frac{0.6}{0.58} = 427.3 m/s$$

$$L_{sl_1} = U_{sl} \Delta W_{u_{sl}} = 324 \cdot 174.4 = 56.5 kJ/kg$$

The work of the HPC last stage is calculated, assuming that the lattice

density at the sleeve $\left(\frac{b}{t}\right)_{sl} = 2.2$

$$c_{1a_c} = 120m/s$$

$$\Delta W_{u_{slz}} = c_{1a_c} \frac{1.55}{1 + 1.5 \frac{t}{b}} = 120 \cdot \frac{1.55}{1 + 1.5 \frac{1}{2.2}} = 110.6 m/s$$

$$u_{1_{slz}} = u_{t_{av}} \frac{D_{slc}}{D_{t_{av}}} = 413 \cdot \frac{0.549}{0.58} = 390.8 m/s$$

$$L_{slz} = U_{slc} \Delta W_{u_{slc}} = 390.8 \cdot 110.6 = 43.2kJ/kg$$

The mean work of the stage: $L_{av} = \frac{56.5+43.2}{2} \approx 49.9 kJ/kg$

The stage number of the HPC is: $z = \frac{L_{hpc}}{L_{av}} = \frac{497}{49.9} \approx 10$ stages

Table 2.2

z	1	2	3	4	5	6	7	8	9	10
L_{st} , kJ/kg	49	52	55	54	53.5	50	48	47	45	43.5
C_a , m/s	180	179	177	173	165	155	145	135	127	120

Distribution of compression work and air axial speed among stages of the compressor are in table 2.2. The number of HPC stages is 10.

2.1.10 Calculation the number of low-pressure compressor stages

$$G_g = G_{a1}(1 + g_f) = 62.4 \cdot (1 + 0.0207) = 63.7 \text{ kg/s}$$

$$L_{lpt} = \frac{mL_{fanII} + L_{fanI}}{(1 + g_f)\eta_m} = \frac{5 \cdot 36 + 48}{(1 + 0.0207) \cdot 0.99} = 265.6 \text{ kJ/kg}$$

we assume $G_g = 64 \text{ kg/s}$, $D_{lptav} = 0.7 \text{ m}$

$$u_{lptmd} = u_{1c} \frac{D_{lptmd}}{D_{1c}} = 500 \cdot \frac{0.7}{1.65} = 212 \text{ m/s}$$

The loading parameter y^* is determined at $z=4$:

$$y^* = u_{lpt} \sqrt{\frac{z\eta_{lpt}^*}{2L_{lpt}}} = 212 \cdot \sqrt{\frac{4 \cdot 0.91}{2 \cdot 265600}} = 0.555$$

2.1.11 Calculation of parameters at the low-pressure turbine entrance

The gas critical speed in the LPT nozzle diaphragm:

$$C_{cr} = 18.5 \sqrt{T_{hpt}^*} = 18.5 \cdot \sqrt{1055} = 600.9 \text{ m/s}$$

the nozzle diaphragm exhaust gas flow velocity:

$$C_I = \frac{L_{stI}}{u_{tav} \cos \alpha_I} = \frac{106340}{212 \cdot 0.9397} = 533.5 \text{ m/s}$$

$$\lambda_1 = \frac{533.5}{600.9} = 0.887 < 1$$

$$q(\lambda_1) = 0.97$$

The cross-section area at the exit of LPT ND:

$$F_{I_{nd}} = \frac{G_g \sqrt{T_{ti}^*}}{m_g p_{hpt}^* \sigma_{nd} \sigma_{int} q(\lambda_1)_{nd} \sin \alpha_1}$$

$$F_{I_{nd}} = \frac{63.7 \sqrt{1055}}{0.0396 \cdot 6.9 \cdot 10^5 \cdot 0.98 \cdot 0.98 \cdot 0.97 \cdot 0.342} = 0.239 \text{ m}^2$$

the length of ND stator vane:

$$h_b = \frac{F_{I_{nd}}}{\pi D_{tav}} = \frac{0.239}{\pi \cdot 0.706} = 0.114 \text{ m}$$

the outer diameter at the exit of the LPT ND:

$$D_h = D_{lpt} + h_b = 0.706 + 0.11 = 0.816 \text{ m}$$

$$D_{sl} = \sqrt{D_h^2 - \frac{4}{\pi} F_{ndlpt}}$$

$$D_{sl} = \sqrt{0.82^2 - \frac{4}{3.14} 0.239} = 0.596 \text{ m}$$

Finally we get:

$$D_h = 0.82 \text{ m}; D_{sl} = 0.592 \text{ m}; h_b = 114 \text{ mm}$$

2.1.12 Calculation of diameters at the low-pressure turbine exit

$$T_t^* = T_{hpt}^* - \frac{L_{lpt}}{\frac{k_g}{k_g - 1} R_g} = 1055 - \frac{265600}{4 \cdot 288} = 824.4 \text{ K}$$

$$p_t^* = p_{hpt}^* \sigma \left(1 - \frac{T_{hpt}^* - T_t^*}{T_{hpt}^* \eta_{lptd}^*} \right)^{\frac{k_g}{k_g - 1}}$$

$$p_t^* = 6.9 \cdot 10^5 \cdot 0.98 \cdot \left(1 - \frac{1055 - 824.4}{1055 \cdot 0.91} \right)^4 = 2.4 \cdot 10^5 \text{ Pa}$$

The axial gas speed at the exit from the LPT ND:

$$C_{1a} = C_1 \sin \alpha_1 = 533.5 \cdot 0.342 = 182.5 \text{ m/s}$$

The cross-section area at the exit from the LPT:

$$F_t = \frac{G_g \sqrt{T_t^*}}{m_g p_t^* q(\lambda_{2a})}$$

$$F_t = \frac{63.7 \cdot \sqrt{824.4}}{0.0396 \cdot 2.4 \cdot 10^5 \cdot 0.8133} = 0.31 \text{ m}^2$$

$$h_b = \frac{F_t}{\pi D_{tav}} = \frac{0.3}{\pi \cdot 0.708} = 0.14 \text{ m}$$

$$D_t = D_{tav} + h_b = 0.708 + 0.14 = 0.85 \text{ m}$$

$$D_{sl} = \sqrt{D_t^2 - \frac{4}{\pi} F_t} = \sqrt{0.85^2 - \frac{4}{3.14} \cdot 0.31} = 0.567 \text{ m}$$

$$h_b = \frac{D_t - D_{sl}}{2} = \frac{0.85 - 0.567}{2} = 0.1415 \text{ m}$$

at the exit from the LPT we get:

$$P_t^* = 2.4 \cdot 10^5 \text{ Pa} \quad T_t^* = 824.4 \text{ K} \quad D_t = 0.85 \text{ m}$$

$$D_{sl} = 0.567 \text{ m} \quad h_b = 141.5 \text{ mm} \quad \frac{D_{tav}}{h_b} = \frac{0.7}{0.14} = 5$$

2.1.13 Calculation of the turbofan engine jet nozzles

the value of jet nozzle differential pressure:

$$\pi_{jn_1} = \frac{p_{td} \sigma_{jn_1}}{p_{am}} = \frac{1.86 \cdot 0.98}{1.013} = 1.8$$

The exhaust velocity from the nozzle:

$$C_{n1} = \sqrt{2 \cdot \frac{k_g}{k_g - 1} \cdot R_g T_t^* \left(1 - \left(\frac{p_{am}}{p_t^* \sigma_n} \right)^{\frac{k_g - 1}{k_g}} \right)}$$

$$C_{n1} = \sqrt{2 \cdot 4 \cdot 288 \cdot 824.4 \cdot \left(1 - \left(\frac{1.013}{2.4 \cdot 0.98} \right)^{0.25} \right)} = 619.7 \text{ m/s}$$

$$\lambda_{n1} = \frac{C_{n1}}{C_{cr}} = \frac{619.7}{18.15 \cdot \sqrt{824.4}} = 0.9941$$

$$q(\lambda_{n1}) = 1.5774 \cdot 0.9941 \cdot \left(1 - \frac{1}{6} 0.9941^2 \right)^{2.5} = 1$$

The area and diameter of the nozzle:

$$F_n = \frac{G_g \sqrt{T_t^*}}{m_g p_t^* \sigma_n q(\lambda_{n1})}$$

$$F_{n1} = \frac{62.4 \cdot \sqrt{824.4}}{0.0396 \cdot 2.4 \cdot 10^5 \cdot 0.98 \cdot 1} = 0.199 \text{ m}^2$$

$$D_{n1} = \sqrt{\frac{4F_{n1}}{\pi}} = \sqrt{\frac{4 \cdot 0.199}{3.14}} = 0.503 \text{ m}$$

The exhaust velocity from the nozzle outer contour $c_c = 280.2 \text{ m/s}$

Reduced velocity and relative density of the flow:

$$\lambda_{n2} = \frac{C_{n2}}{C_{cr}} = \frac{280.2}{18.15 \cdot \sqrt{340}} = 0.84$$

$$q(\lambda_{n2}) = 1.5774 \cdot 0.84 \left(1 - \frac{1}{6} 0.84^2\right)^{2.5} = 0.97$$

The area of the nozzle cross-section:

$$F_{n2} = \frac{G_{aII} \sqrt{T_{fanII}^*}}{m_a p_{n2}^* \sigma_{n2} q(\lambda_{n2})}$$

$$F_{n2} = \frac{312 \cdot \sqrt{333.5}}{0.040348 \cdot 1.822 \cdot 10^5 \cdot 0.98 \cdot 0.97} = 0.791 \text{ m}^2$$

the external diameter of nozzle:

$$D_{n2} = \sqrt{D_{in}^2 + \frac{4F_{n2}}{\pi}} = \sqrt{0.91^2 + \frac{4 \cdot 0.791}{3.14}} = 1.355 \text{ m}$$

Table 2.3

TFE Elements	Number of stages	Element parameters			Cross-sections	Working b
		G,kg/s	n,rpm	N,kW		p*,Pa
Fan(outer duct)	1	312	5788	14255	Inlet	1.01×10^5
					Exit	1.60×10^5
LPC(inner duct)	3	62.41	5788	2496	Inlet	1.52×10^5
					Exit	2.43×10^5
HPC	10	60.5	13601	30748	Inlet	2.38×10^5
					Exit	32.0×10^5
HPT	1	61.2	13601	31059	Inlet	30.8×10^5
					Exit	6.9×10^5
LPT	4	63.7	5788	16935	Inlet	6.9×10^5
					Exit	2.395×10^5
Nozzle II		312			Exit N II	1.86×10^5
Nozzle I		63.7			Exit N I	1.82×10^5

Chapter 3 Gas-dynamic Calculation Of The Axial Turbine Stage And Turbine Rotor Blade Strength Calculation

3.1 Gas-dynamic Calculation of the axial turbine stage

gas pressure at the entry to the high-pressure turbine:

$$p_g^* = p_0^* = 30.8 \cdot 10^5 Pa$$

gas temperature at the entry to the high-pressure turbine:

$$T_g^* = T_0^* = 1500 K$$

mass gas flow rate:

$$G_g = 60.5 kg/s$$

HPT stage work:

$$L_{st} = 507000 J/kg$$

circumferential velocity on the middle radius:

$$u_{md} = 413 m/s$$

angle of the stream output from nozzle diaphragm: $\alpha_1 = 20^\circ$

external, middle and sleeve diameters at the entry to the working wheel:

$$D_{1K} = 0,63 m, D_{1sl} = 0,570 m, D_{1md} = 0,6 m$$

jet velocity of gas at the exit from the nozzle diaphragm:

$$c_1 = 696 m/s$$

reduced velocity at the nozzle diaphragm exit: $\lambda_1 = 0,93$

pressure recovery coefficient in the nozzle diaphragm: $\sigma_{ND} = 0,98$

Section area at the inlet HPT first stage working wheel:

$$F_1 = \frac{G_g \sqrt{T_g^*}}{m_g p_g^* \sigma_{ND} q(\lambda_{c_1}) \sin \alpha_1}$$

For $\lambda_1 = 0.93$ relative density $q(\lambda_{c_1}) = 0.994$

$$F_1 = \frac{60.5\sqrt{1500}}{0.0396 \cdot 30.8 \cdot 10^5 \cdot 0.98 \cdot 0.994 \cdot \sin 20^\circ} = 0.057 m^2$$

blade height:

$$h_1 = \frac{F_1}{\pi D_{1md}} = \frac{0.057}{3.14 \cdot 0.6} = 0.0303 m$$

external diameter:

$$D_{1K} = D_{1md} + h_1 = 0.6 + 0.0303 = 0.6303 m$$

sleeve diameter:

$$D_{1sl} = D_{1md} - h_1 = 0.6 - 0.0303 = 0.57 m$$

relative sleeve diameter:

$$\bar{d}_{sl} = \frac{D_{1sl}}{D_{1K}}, \bar{d}_{sl} = \frac{0.57}{0.63} = 0.905$$

Gas temperature at the exit from the turbine stage:

$$T_2^* = T_0^* - \frac{L_{st}}{\frac{k_g}{k_g - 1} R_g}$$

$$T_2^* = 1500 - \frac{270000}{\frac{1.33}{1.33 - 1} 288} = 1317 K$$

Gas pressure at the exit from the turbine stage:

$$p_2^* = p_0^* \left(1 - \frac{T_0^* - T_2^*}{T_0^* \eta_{st}}\right)^{\frac{k_g}{k_g - 1}}$$

$$p_2^* = 30.8 \cdot 10^5 \left(1 - \frac{1500 - 1317}{1500 \cdot 0.91}\right)^{\frac{1.33}{1.33 - 1}} = 14.9 \cdot 10^5 Pa$$

Axial component of the jet velocity:

$$c_{2a} = c_{1a} + \Delta c_a, \Delta c_a = 40 \text{ m/s}$$

$$c_{1a} = c_1 \sin \alpha_1 = \lambda_{c_1} 18,15 \sqrt{T_g^*} \sin \alpha_1, c_{1a} = 0,93 \cdot 18,15 \sqrt{1500} \sin 20^\circ = 227,3 \text{ m/s}$$

$$c_{2a} = 332,5 + 40 = 267,3 \text{ m/s}$$

Reduced velocity:

$$\lambda_{c_{2a}} = \frac{c_{2a}}{18,15 \sqrt{T_2^*}}, \lambda_{c_{2a}} = \frac{267,3}{18,15 \sqrt{1317}} = 0,41$$

Section area at the exit from the working wheel:

$$F_2 = \frac{G_g \sqrt{T_2^*}}{m_g p_2^* q(\lambda_{c_{2a}})}$$

$$F_2 = \frac{60,5 \sqrt{1317}}{0,0396 \cdot 14,9 \cdot 10^5 \cdot 0,6055} = 0,087 \text{ m}^2$$

we assume $D_{1K} = D_{2K} = 0,63 \text{ m}$

Diametric dimensions at the working wheel exit:

$$D_{2sl} = \sqrt{D_{2K}^2 - \frac{4F_2}{\pi}} \quad D_{2sl} = \sqrt{0,63^2 - \frac{40 \cdot 0,087}{3,14}} = 0,56 \text{ m}$$

$$D_{2md} = \frac{D_{2K} + D_{2sl}}{2} \quad D_{2md} = \frac{0,63 + 0,56}{2} = 0,595 \text{ m}$$

$$h_2 = \frac{D_{2K} - D_{2sl}}{2} \quad h_2 = \frac{0,63 - 0,56}{2} = 0,035 \text{ m}$$

stage loading coefficient on the middle radius:

$$\mu_{md} = \frac{L_{st}}{u_{md}^2} \quad \mu_{md} = \frac{270000}{413^2} = 1,58$$

Absolute velocity and reduced velocity at the exit from the nozzle

diaphragm is axial flow output:

$$c_{2u} = 0$$

$$c_{1md} = \frac{L_{st}}{u_{md} \cos \alpha_1} \quad c_{1md} = \frac{270000}{413 \cos 20^\circ} = 695.7 \text{ m/s}$$

$$\lambda_{c_{1md}} = \frac{c_{1md}}{18.15\sqrt{T_1^*}} \quad \lambda_{c_{1md}} = \frac{695.7}{18.15\sqrt{1550}} = 0.97$$

Axial component of the jet velocity and parameter \bar{c}_{1a} at the entry to the working wheel:

$$c_{1a} = c_1 \sin \alpha_1; \quad c_{1a} = 695.7 \sin 20^\circ = 225.4 \text{ m/s}$$

$$\bar{c}_{1a} = \frac{c_{1a}}{u}; \quad \bar{c}_{1a} = \frac{225.4}{413} = 0.546$$

Circumferential components of the jet velocity at the entry to the working wheel:

$$c_{1u} = c_1 \cos \alpha_1; \quad c_{1u} = 695.7 \cos 20^\circ = 653.75 \text{ m/s}$$

$$c_{2u} = \frac{L_{st}}{u_{md}} - c_{1u}; \quad c_{2u} = 0 \text{ m/s}$$

$$c_{u_m} = \frac{c_{1u} - c_{2u}}{2}; \quad c_{u_m} = \frac{653.75 - 0}{2} = 327 \text{ m/s}$$

$$\bar{c}_{1u} = \frac{c_{1u}}{u_{md}}; \quad \bar{c}_{1u} = \frac{653.75}{413} = 1.54$$

$$\bar{c}_{2u} = \frac{c_{2u}}{u_{md}}; \quad \bar{c}_{2u} = 0$$

Relative gas velocity and its circumferential component:

$$w_{1umd} = c_{1umd} - u_{md}; \quad w_{1umd} = 653.75 - 413 = 240.75 \text{ m/s}$$

$$w_{1md} = \sqrt{c_{1amd}^2 + w_{1umd}^2}; \quad w_{1md} = \sqrt{225.4^2 + 240.75^2} = 329.8 \text{ m/s}$$

Angle of the stream inlet into the working wheel in the relative direction:

$$\beta_1 = \operatorname{arctg} \frac{c_{1a}}{w_{1u}} \quad \beta_1 = \operatorname{arctg} \frac{225.4}{240.75} = 43^\circ$$

Jet velocity and reduced velocity at the exit from the working wheel:

$$c_2 = \sqrt{c_{2a}^2 + c_{2u}^2} \quad c_2 = \sqrt{267.3^2 + 0^2} = 267.3 \text{ m / s}$$

$$\lambda_{c_2} = \frac{c_2}{18,15\sqrt{T_2^*}} \quad \lambda_{c_2} = \frac{267.3}{18,15\sqrt{1317}} = 0.41$$

Stream output angle at the exit from the working wheel in the relative direction:

$$\beta_2 = \operatorname{arctg} \frac{c_{2a}}{c_{2u} + u} \quad \beta_2 = \operatorname{arctg} \frac{267.3}{0 + 413} = 32.9^\circ$$

Relative velocity at the exit from the working wheel and its circumferential component:

$$w_2 = \frac{c_{2a}}{\sin \beta_2} \quad w_2 = \frac{267.3}{\sin 32.9^\circ} = 492 \text{ m / s}$$

$$w_{2u} = w_2 \cos \beta_2 \quad w_{2u} = 492 \cos 32.9^\circ = 413.1 \text{ m / s}$$

Stagnated temperature and critical gas velocity in the relative direction:

$$T_{w_1}^* = T_{w_2}^* = T_0^* - \frac{k_g - 1}{2k_g R_g} (c_1^2 - w_1^2)$$

$$T_{w_1}^* = 1500 - \frac{1.33 - 1}{2 \cdot 1.33 \cdot 288} (695.7^2 - 329.8^2) = 1388 \text{ K}$$

$$a_{crw} = 18,15\sqrt{T_{w_1}^*} \quad a_{crw} = 18,15\sqrt{1388} = 676.2 \text{ m / s}$$

$$\text{Airtwist} \quad \Delta w_u = w_{1u} + w_{2u}$$

$$\Delta w_u = 240.75 + 413 = 653.85 \text{ m / s}$$

Reduced velocities at the entry to the working wheel and behind turbine stage:

$$\lambda_{w_1} = \frac{w_1}{a_{crw}} ; \lambda_{w_1} = \frac{329.8}{676.2} = 0.49$$

$$\lambda_{w_2} = \frac{w_2}{a_{crw}} ; \lambda_{w_2} = \frac{492}{676.2} = 0.73$$

Cinematic reactivity rate:

$$\rho_K = 1 - \frac{c_{1u}}{u} + \frac{\Delta w_u}{2u} ; \rho_K = 1 - \frac{653.85}{413} + \frac{653.85}{2 \cdot 413} = 0.21$$

Circumferential velocities at the entry to the working wheel and behind it

are the same ($u_1 = u_2$). Turbine stage work:

$$L_{st} = \frac{1}{2}(c_1^2 - c_2^2 + w_2^2 - w_1^2)$$

$$L_{st} = \frac{1}{2}(695.7^2 - 267.3^2 + 492^2 - 329.8^2) = 272920 J / kg$$

$$\delta L_{st} = \left| \frac{270000 - 272920}{245000} \right| \cdot 100\% = 1.08\%$$

$\delta L_{st} < 3\%$, so the result is accepted.

$$\rho_{sl} = 1 - (1 - \rho_{md}) \left(\frac{D_{md}}{D_{sl}} \right)^{m+1}$$

$$\rho_{sl} = 1 - (1 - 0.21) \left(\frac{0.6}{0.57} \right)^{1+1} = 0.125 > 0$$

we choose law of circulation constancy across the radius $c_{u_m} r = const$.

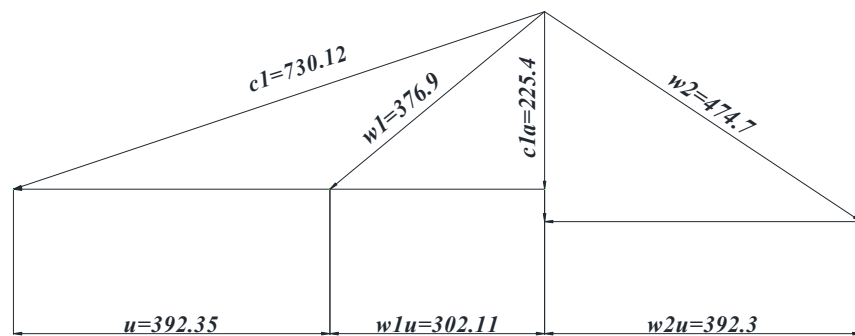
Table3.1

Parameters	Section		
	sleeve	middle	peripheral
D, m	0.57	0.6	0.63

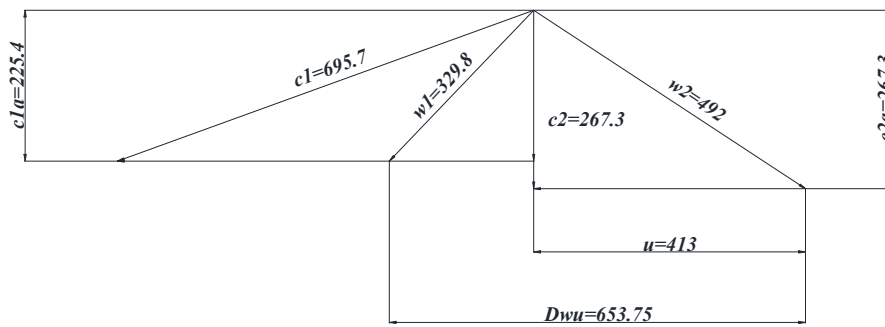
$u = u_{md} \frac{D}{D_{md}}, \text{ m/s}$	392.35	413	433.65
$\mu = \frac{L_{st}}{u^2}$	1,77	1,6	1,45
$c_{1a} = c_{1amd} = const, \text{ m/s}$	225.4	225.4	225.4
$c_{1u}, \text{ m/s}$	694.46	653.75	628.8
$c_1 = \sqrt{c_{1a}^2 + c_{1u}^2}, \text{ m/s}$	730.12	695.7	668
$\lambda_{c_1} = \frac{c_1}{18,15\sqrt{T_1^*}}$	0.97	0.93	0.896
$\alpha_1 = \text{arctg} \frac{c_{1a}}{c_{1u}}, \text{ deg}$	18.0	19	19.7
$w_{1u} = c_{1u} - u, \text{ m/s}$	302.11	240.75	195.15
$w_1 = \sqrt{c_{1a}^2 + w_{1u}^2}, \text{ m/s}$	376.9	329.8	298.14
$\beta_1 = \text{arctg} \frac{c_{1a}}{w_{1u}}, \text{ deg}$	36.7	43	49.1
$c_{2a} = c_{1amd} = const, \text{ m/s}$	267.3	267.3	267.3
$c_{2u}, \text{ m/s}$	0	0	0
$c_2 = \sqrt{c_{2a}^2 + c_{2u}^2}, \text{ m/s}$	267.3	267.3	267.3
$\alpha_2 = \text{arctg} \frac{c_{2a}}{c_{2u}}, \text{ deg}$	90	90	90
$\lambda_{c_2} = \frac{c_2}{18,15\sqrt{T_2^*}}$	0.41	0.41	0.41
$\beta_2 = \text{arctg} \frac{c_{2a}}{c_{2u} + u}, \text{ deg}$	34.27	32.9	31.65
$w_2 = \frac{c_{2a}}{\sin \beta_2}, \text{ m/s}$	474.7	492	509.4

$w_{2u} = w_2 \cos\beta_2, \text{ m/s}$	392.3	413	433.64
$T_{w_1}^* = T_0^* - \frac{k_g - 1}{2k_g R_g} (c_1^2 - w_1^2), \text{ K}$	1382	1388	1396
$\lambda_{w_1} = \frac{w_1}{a_{crw}}$	0.557	0.49	0.441
$\lambda_{w_2} = \frac{w_2}{a_{crw}}$	0.7	0.73	0.75
$\rho_K = 1 - \frac{c_{1u}}{u} + \frac{\Delta w_u}{2u}$	0.16	0.21	0.24
$L_{st} = \frac{1}{2} (c_1^2 - c_2^2 + w_2^2 - w_1^2), \text{ J/kg}$	272460	272920	272690
$\delta L_{st} = \frac{L_{stu} - L_{st}}{L_{stu}} 100, \%$	0.9	1.08	1

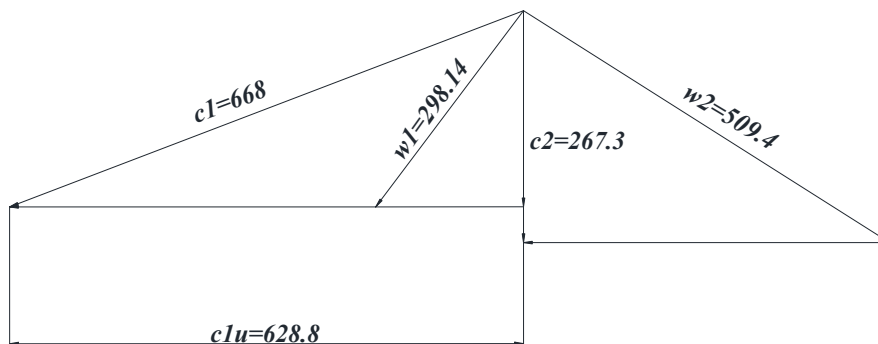
speed plans for three sections on blade height:



(1)



(2)



(3)

Fig.3.1 Axial turbine stage speed plans:

(1) – sleeve section; (2) – middle section; (3)– peripheral section.

3.2 Turbine rotor blade strength calculations

We choose the structural element with the highest load on the rotor of the gas turbine engine - the rotor blade of the high pressure turbine as the object of the strength calculation[8].

Supplementary data:

Specific heat of gas $c_{pg}=1160 \text{ J}/(\text{kg}\cdot\text{K})$

Isotropic exponent $K_g=1.33$

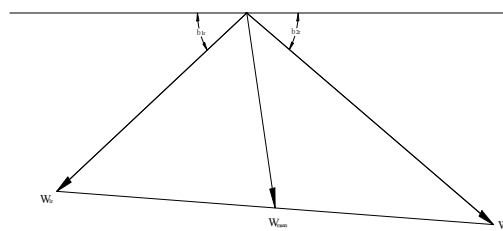
Gas constant $R_x=288 \text{ J}/(\text{kg}\cdot\text{K})$

The number of high-pressure compressor (HPC) stages $z=10$

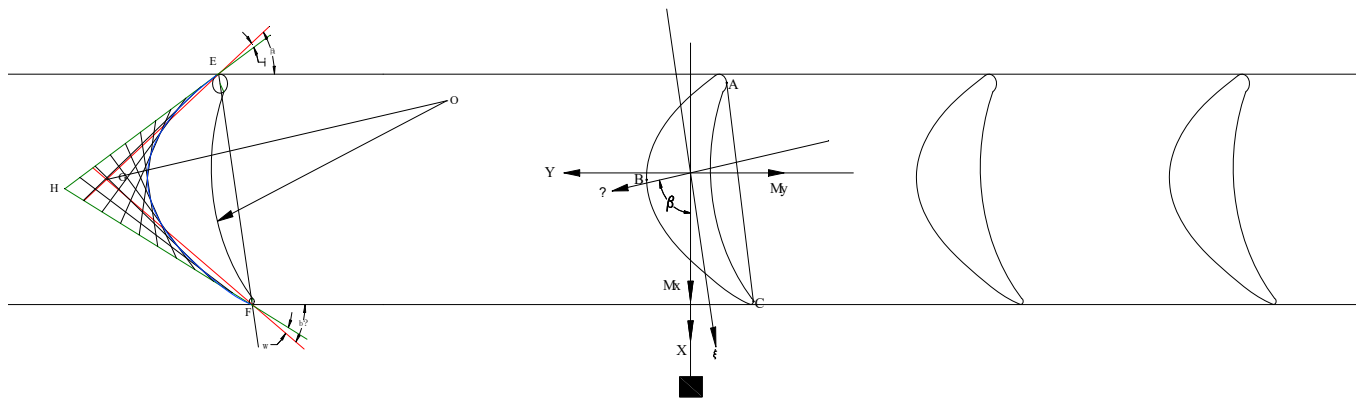
The centrifugal forces cause tensile, bending and torsion deformations, gas forces cause bending and torsion of blades.

The turbine blade root section, middle section and peripheral section. The turbine blade twisted from root section to peripheral section according to the optimal designed angle.

Scale 1cm:50 m/s

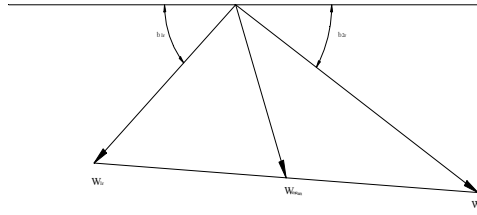


Scale 2:1

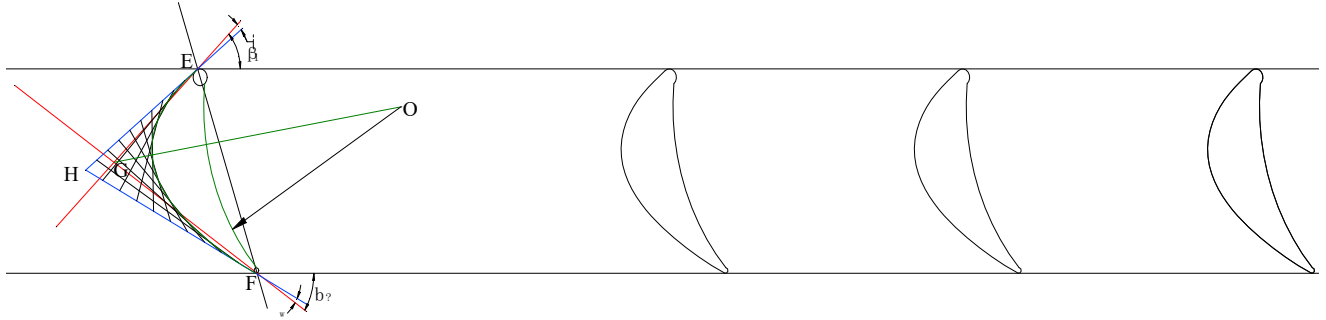


(1)sleeve section

Scale 1cm:50 m/s

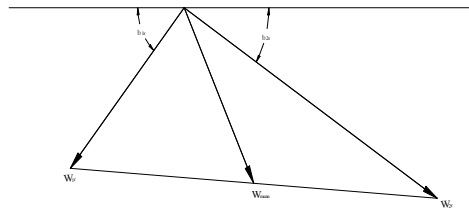


Scale 2:1

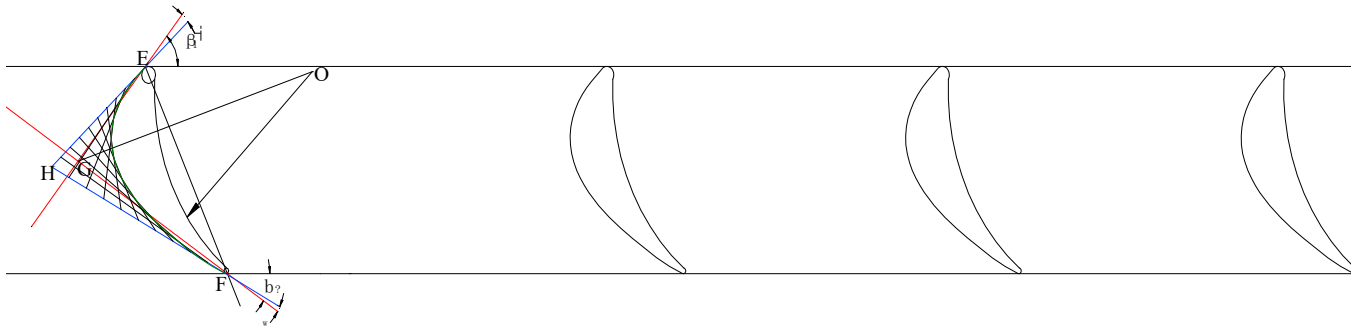


(2)middle section

Scale 1cm:50 m/s



Scale 2:1



(3)peripheral section

Fig 3.2 geometrical characteristics of three sections

The initial data for HPT rotor blade strength calculation are in Table 3.2

Table 3.2

Parameters	designation	value
Relative velocity of gas at the rotor wheel inlet, m/s	W_1	376.9
Angle of gas relative velocity at the rotor wheel inlet, deg.	β_1	36.7
Relative velocity' of gas at the rotor wheel discharge, m/s	W_2	474.7
Angle of gas relative velocity at the rotor wheel discharge, deg.	β_2	34.27
Axial length of turbine rotor blade profile in root section, m	l	$1.59 \cdot 10^{-2}$
Radius of turbine rotor blade root section, m	r_r	$1.31 \cdot 10^{-2}$
Radius of turbine rotor blade tip section, m	r_0	$1.71 \cdot 10^{-2}$
Relative area of turbine rotor blade tip section, m^2	F	$8 \cdot 10^{-5}$
Rotational speed of turbine rotor, r/min (rpm)	n_{HP}	13600
Gas flow rate through the turbine, kg/s	G_g	60.5
Quantity of rotor blades in the turbine rotor wheel	z_b	72
Static pressure of gas at the turbine rotor wheel inlet, MPa	P_{nd}	$3.1 \cdot 10^6$
Static pressure of gas at the turbine rotor wheel discharge, MPa	P_{td}	$1.5 \cdot 10^6$
Temperature of turbine rotor blade root section	T_b	1388
Internal diameter of turbine rotor wheel inlet, m	d_{nd}	0.65
Internal diameter of turbine rotor wheel discharge, m	d_{td}	0.64
External diameter of turbine rotor wheel inlet, m	D_{nd}	0.72
External diameter of turbine rotor wheel discharge, m	D_{td}	0.75
Moment of inertia of turbine rotor blade root section relative to ξ axis, $N \cdot m$	J_ξ	$1.04 \cdot 10^{-9}$
Moment of inertia of turbine rotor blade root section relative to η axis, $N \cdot m$	J_η	$0.75 \cdot 10^{-9}$
Angle between axes x and η . deg.	β	80°
Coordinate of a point A relative to ξ axis, m	ξ_A	$3.19 \cdot 10^{-3}$

Coordinate of a point B relative to ξ axis, m	ξ_B	$3.19 \cdot 10^{-3}$
Coordinate of a point C relative to ξ axis, m	ξ_C	$4.22 \cdot 10^{-3}$
Coordinate of a point A relative to η axis, m	η_A	$5.56 \cdot 10^{-3}$
Coordinate of a point B relative to η axis, m	η_B	$0.22 \cdot 10^{-3}$
Coordinate of a point C regarding to η axis, m	η_C	$9.7 \cdot 10^{-3}$
Axial length of a tip shroud cap, m	b'	$1.67 \cdot 10^{-2}$
Thickness of a shroud cap, m	δ_c	0.002

3.2.1 Tensile stresses in blade root caused by centrifugal forces

Tensile stress in blade root section:

$$\begin{aligned}\sigma_{tens.r} &= 4\rho_b U_{mean1}^2 \frac{h}{D_{nd} + d_{nd}} \left[1 - \frac{2(1 - \bar{F})}{(1 + m)(2 + m)} \left(1 + \frac{mD_{nd}}{D_{nd} + d_{nd}} \right) \right] \\ &= 4 \cdot 8200 \cdot U_{mean1}^2 \frac{h}{D_{nd} + d_{nd}} \left[1 - \frac{2(1 - \bar{F})}{1.5 \cdot 2.5} \left(1 + \frac{mD_{nd}}{D_{nd} + d_{nd}} \right) \right] \\ &= 273.554 MPa\end{aligned}$$

Shroud cap mass:

$$M_c = \frac{\pi(D_{nd} + D_{td}) \cdot 0.8l \cdot 0.002 \cdot \rho_b}{2Z_b} = 6.69 \cdot 10^{-3} Kg$$

where 0.002 is shroud cap thickness, m

The diameter of shroud cap center of weight:

$$D_{c.c} = \frac{D_{nd} + D_{td}}{2} + 0.002 = 0.737m$$

Centrifugal force of rotating weight of shroud cap:

$$P_{c.c} = M_c \cdot \left(\frac{\pi n_{HP}}{30} \right)^2 \cdot \frac{D_{c.c}}{2} = 5 \cdot 10^6 N$$

Area of rotor blade root section:

$$F_r \approx 0.7bc_{max} = 7.6 \cdot 10^{-5} \text{m}^2$$

Tensile stress in rotor blade root section:

$$\sigma_{tens.r\Sigma} = \frac{(\sigma_{tens.r} \cdot F_r \cdot 10^6 + P_{c.c}) \cdot 10^{-6}}{F_r} = 339.35 \text{MPa}$$

3.2.2 Bending stresses caused by gas forces

The bending stresses caused by gas forces are calculated for points A, B, C of rotor blade root section.

The intensity of gas loads along axes x and y:

$$q_x = \frac{\pi(D_{nd} + d_{nd})[\rho_b c_{nda}(c_{nda} - c_{tda}) + (P_{nd} \cdot 10^6 - P_{td} \cdot 10^6)]}{2Z}$$

$$= 4.82 \cdot 10^4 \text{N/m}$$

$$q_y = \frac{\pi(D_{nd} + d_{nd})\rho_{nd}c_{1a}(c_{1u} - c_{2u})}{2Z} = 8.89 \cdot 10^3 \text{N/m}$$

The bending momenta with respect to axes x and y:

$$M_x = \frac{q_y h^2}{2} = 5.5 \text{ N} \cdot \text{m}; \quad M_y = \frac{q_x h^2}{2} = 30 \text{ N} \cdot \text{m}$$

The bending momenta with respect to main axes of inertia:

$$M_\xi = M_x \sin \beta + M_y \cos \beta = 10.63 \text{ N} \cdot \text{m}$$

$$M_\eta = M_x \cos \beta - M_y \sin \beta = -28.589 \text{ N} \cdot \text{m}$$

The bending stresses caused by gas forces, acting in points A,B,C

$$\sigma_{bA} = + \left(\frac{M_\xi \eta_A}{J_\xi} \right) - \left(\frac{M_\eta \xi_A}{J_\eta} \right) = 218.12 \text{MPa}$$

$$\sigma_{bB} = - \left(\frac{M_\xi \eta_B}{J_\xi} \right) + \left(\frac{M_\eta \xi_B}{J_\eta} \right) = -145.12 \text{MPa}$$

$$\sigma_{bC} = - \left(\frac{M_\xi \eta_C}{J_\xi} \right) + \left(\frac{M_\eta \xi_C}{J_\eta} \right) = 45.52 \text{MPa}$$

The total stresses in points A.,B, C:

$$\sigma_{\Sigma A} = \sigma_{tens.r\Sigma} + \sigma_{b A} = 557.47 \text{ MPa}$$

$$\sigma_{\Sigma B} = \sigma_{tens.r\Sigma} + \sigma_{b B} = 194.23 \text{ MPa}$$

$$\sigma_{\Sigma C} = \sigma_{tens.r\Sigma} + \sigma_{b C} = 384.87 \text{ MPa}$$

strength safety factors:

$$K_A = \frac{\sigma_{100}^{T_{br}}}{\sigma_{\Sigma A}} = 1.53$$

$$K_B = \frac{\sigma_{100}^{T_{br}}}{\sigma_{\Sigma B}} = 4.38$$

$$K_C = \frac{\sigma_{100}^{T_{br}}}{\sigma_{\Sigma C}} = 2.21$$

Where $\sigma_{100}^{T_{br}}=850\text{MPa}$, by adoption of Ni-based alloy Rene’N6[9].

Conclusion:

As the results of calculation show, strength safety factors $K_A, K_B, K_C > 1.5$,

it means that the turbine blade strength is acceptable.

Chapter 4 LABOR PROTECTION

4.1 Introduction

The topic of my diploma work is generally about improvement performances of a bypass engine .So the key point of this labor protection research part content is occupational safety and health measures for protection of engineer on aviation maintenance developed program works on the engine.

4.2 Harmful and hazardous working factors

Labor protection measures in a specific workplace, indoors or in a specific service are determined by the degree of safety of each process. The safety and reliability of each process can be determined by the number of dangerous and harmful factors and the severity of each harmful factor. In the site where work is carried out, many hazards and factors can affect the people who work in it[11].

The most important first step, we need to list the possible dangerous and harmful factors. This includes the operation, disassembly, storage, assembly, transfer, etc. of equipment on the aircraft or in the aircraft maintenance site.

Listed below are some of the factors that can have a detrimental effect on people at work in a place:

- Movable mechanical equipment, special equipment.
- There are no protected moving parts in the machinery.

- Fragmentation of parts that may occur in production.
- Dropping of equipment parts when working at heights with a lift.
- Gases and liquids discharged from pipes under pressure.
- Containers operating under hydraulic and pneumatic pressure may fluctuate.
- Dust and gaseous pollutants from aircraft maintenance areas.
- Noise, vibration sound waves, ultrasonic waves, etc.
- Radiation from certain workplaces.
- Sharp spots exposed on the surface of the aircraft fuselage.
- Insufficient ambient lighting, resulting in dim vision.

The maximum allowable noise value for a particular aircraft needs to be clearly specified. ICAO standards set standards for noise produced by aircraft over three time periods: when the aircraft takes off, when the aircraft is climbing, and before the aircraft lands [10].

The climatic condition of the workplace generally refer to the fact that at the worker's own heat expenditure and absorption tend to balance under certain circumstances. In autumn and winter, the suitable temperature is about 20 degrees Celsius, and in the warmer spring and summer, the temperature is slightly higher, about 25 degrees Celsius. Temperature disturbances in the workplace may be due to inadequate ventilation or a malfunction of the regulation system.

4.3 Analysis of working conditions and development of protective measures

In order to reduce the influence of dangerous and adverse factors, according to the requirements of maintenance operation safety, the following improvement measures are listed:

- ◆ The aircraft parking positions are clearly marked.
- ◆ Around the movement and parking of aircraft, organize the operation of other means of transportation according to regulations.
- ◆ The maximum speed on the tarmac is 20 kilometers per hour.
- ◆ The staff of aircraft fuel tanks need to wear professional masks, respiratory masks and other protective measures at work.
- ◆ During maintenance work, group units can be set up, teamwork can better cope with emergencies.
- ◆ When the engine is running, there will be a lot of noise, and the staff needs professional noise canceling earphones or sound isolating device. Long-term exposure to noise, vibration and ultrasonic working environment will damage the human hearing, brain, nervous system, heart and other organs, which will lead to serious occupational diseases over time.

4.4 Fire Safety Rules at the workspace

In civil aviation airports, fire safety is mainly divided into two categories: fire safety for flight maintenance and fire safety for aircraft equipment and objects[12].

The goal of flight fire safety is the safety of passengers on board. The fire protection of aviation equipment and objects is the prevention of fire, the evacuation of personnel in the event of a fire, and the protective actions of equipment, such as fuel storage rooms with fire protection facilities.

Airlines can configure more complete fire safety equipment, popularize correct fire protection, guide the safe use of fire extinguishers, and provide vocational training for personnel, etc.

ICAO fire safety issues have been regulated in Annex 14 of the Convention on International Civil Aviation and the Airport Services Manual. According to the above mentioned documents, ICAO Member States require fire safety equipment and services at airports[13]:

- Requirements for the fire rating of airports.
- Time requirements for implementing fire rescue.
- Communication and Reporting Facility Requirements.
- Requirements for the physical condition of fire rescue personnel.

In airports, air bases, maintenance plants and other buildings, the hangar is the place with the highest potential index of danger. Therefore, ac

According to the regulations on fire prevention, it is necessary to use high temperature-resistant thermal insulation materials as walls or protection.

In a fire, the fire spread on the ground floor area is extremely dangerous, the fire will quickly spread to the upper floors, and the smoke generated is also a great harmful factor. Therefore, it is very necessary to have emergency lifts and water spray systems, and these devices need to be placed in places where they can be easily stored and accessed.

The following are the risk factors for people in a fire:

- The burning flame
- The rapidly rising ambient temperature
- The toxic substances produced by the combustion
- The thick black smoke
- The rapid decrease in the oxygen concentration
- The burning structure falling from above

Improve the safety factor of the workplace and prevent the environment from burning and even leading to explosions, which can be improved by the following ways:

- Reduce the use of flammable substances in equipment.
- Provide necessary ventilation to the workplace.
- Avoid use of materials that will react chemically during combustion.
- Make improvements in the production process of industrial equipment

4.5 Special requirement for precaution during maintenance of engine

In popular belief, the prevention of aircraft accidents is about improving operational safety, but in fact, maintenance and troubleshooting errors should also receive more focus.

Airworthiness of an aircraft is a major factor in the safety of aircraft operation, so maintenance of systems, inspection of components, refurbishment of certain areas and accident prevention need to be planned well in advance.

Safety issues mentioned in the aircraft maintenance environment are partly occupational safety and health issues (OSH) and partly ensuring that aircraft maintenance technician provide an airworthiness plan for the flight.

Many fault conditions are latent and not easily detected. For example, it takes a long time for undetected fatigue cracks to gradually evolve into failures. During this latent time, other potential risk factors may continue to be generated. Therefore, in addition to strengthening the aircraft system, other measures such as equipping professional equipment with experienced mechanic, airworthiness directive, fill in the work inspection card carefully, keep a complete record of the inspection process.

4.6 Occupational Safety and Health Protections

Due to the dangerous nature of the working environment, there may be irritating factors such as radioactivity and chemical corrosion. It is necessary to provide workers with physical protective equipment to reduce or avoid health damage to workers[14].

4.6.1 Face protection

If there are flying objects, liquid splashes, strong light situations during operation, workers should be provided with face protection especially eye protection. Eye protection equipment should have the following characteristics:

- sufficient design strength to prevent hazards
- durable and multi-use
- comfortable for users to wear
- light and easy to carry.

4.6.2 Head protection

Wear a helmet to prevent objects from falling. The weight of the helmet should not exceed 0.45 kg. The properties of the helmet are different in different working environments. It should be waterproof in a humid environment, not conductive in an electrical environment, and heat-resistant materials in a high-temperature environment. For proper selection, design, testing and use of helmet, the American National Standard Industrial Head Protection Safety Requirements(ANSI z59-1-1969)are used.

4.6.3 Respiratory protection

The use of respirators is due to the possible presence of dust, fumes, vapors, etc. in the work environment. In particular, it is necessary to correctly select the appropriate respirator according to the type of work of the staff, provide sufficient guidance to the staff, regularly clean and disinfect the respirator. At the same time, companies need to develop standards for the use of respirators to ensure that workers can utilize them correctly during routine operations and emergencies. For correct choose, design, production and use of respirators, the American National Standards Practices for Respiratory Protection (ANSI z88.-21059) is adopted.

4.6.4 Body protection

The first is hand protection, the correct choice of gloves can help workers work more efficiently. For workers with sharp-edged objects in the work process, the gloves should be made of tough materials. When working in high temperature environments, the gloves they wear should be heat-resistant. Electrical gloves are usually made of rubber or other non-conductive materials, and gloves that may contact with corrosive liquids are generally made of corrosion-resistant natural rubber.

When workers are working above mobile machinery, at heights of 20 feet above from the horizontal requires use of safety belts and lifelines.

Conclusion

One of the most important factor during the researches on Branch Labor Precaution is the working condition at the work place and how to provide the most comfort conditions for workers, so the working condition in the work place must fit the norm of ICAO safety management system (SMS) standard according to the requirements.

Chapter 5 ENVIRONMENT PROTECTION

5.1 Introduction

Transport is one of the most important elements of the economic system of each country and at the same time belongs to the group of major environmental pollutants. Among the different modes of transport, air transport has experienced the fastest growth. Air transport as an integral part of the entire transport system of the world has certain advantages compared with land and water transport.

Humans have always affected the natural environment, and many of our actions produce large amounts of waste, including solid, liquid and gaseous residues. Different types of waste enter the cycle of the biosphere, resulting in various kinds of pollution, which have a bad impact on the environment and even on our own human beings.

Aircraft burning fuel pollutes the air, and the fuel itself has serious effects on the soil. In terms of physiology, the operation of the aircraft is the main source of noise, and it also causes certain factors to affect the human body.

For the effects mentioned above, ICAO has established normative standards for the noise level and emissions of aircraft engines.

5.2 The emissions of greenhouse gases in aviation

The climate problem we are now familiar with is global warming, which refers to the increase in the average temperature of the Earth's atmosphere and oceans from the late 19th century to the present. The main cause of global warming is the huge production of greenhouse gases by human activities, the burning of fossil fuels and excessive deforestation.

In 1977, the ICAO was organized the Committee for aircraft engine emissions. Its experts have developed emission limits in exhaust gases of harmful substances, and in 1981, these norms adopted by the Council of ICAO. The rules specify the limit of carbon monoxide (CO), incompletely burnt hydrocarbons (HB), and nitrogen oxides (NO_x) [15].

Emission from aircraft includes:

- Carbon monoxide CO
- Carbon dioxide CO₂
- Nitrogen oxides NO_x
- Sulphur oxides SO_x
- Hydrocarbons C_xH_y
- Smoke
- Benzopyrene

Among them, CO, NO_x and C_xH_y are the main gases, because they have the highest content. So later we will explain the impact of these three components on the polluted atmospheric environment.

The CO and CxHy in the exhaust gas are caused by incomplete combustion of the fuel in the combustion chamber. The degree of fuel combustion in the engine depends on the performance of the engine, or there is a concept called the complete combustion coefficient(η). The fuel burns to the greatest extent when the plane takes off, about 0.96-0.99. In other modes, it will be reduced to 0.7-0.85, at which time the aircraft releases more pollutants.

Engine modes:

- ① Start, idle running before takeoff (regime of low gas)
- ② Takeoff
- ③ Climbing
- ④ Approach landing from a height of 1000 m
- ⑤ Landing taxiing (regime of low gas)

Content of NO_x in the exhaust gases of aircraft engine depends on:

- the temperature of air and fuel mixture in the combustor
- the dwelling time of air and fuel mixture in the combustor

The higher temperature, the more NO_x emissions. There is the highest temperature (2700–3500K) at the takeoff regime of aircraft engine. The less is speed of aircraft, the dwelling time is more, that's why NO_x emissions are the most at the takeoff regime.

The quantitative feature of engine exhaust emissions is the emission index(EI), which expresses the mass of harmful substances emitted into the air per kilogram of fuel after combustion.[EI]=g/kg.

During the determining of emission index first of all control emission parameter of engine M/R_0 , g/kN is determined. This parameter characterized the level of damage of engine. ICAO standards are determined according to this control emission parameter.

M – mass of harmful substances, g

R_0 – maximum thrust of engine, kN

The following are the emission standards stipulated by ICAO:

$$M_{CO} /R_0 = 118 \text{ g/kN}$$

$$M_{C_xH_y} /R_0 = 19.6 \text{ g/kN}$$

$$M_{NO_x} /R_0 = (40...80) \text{ g/kN}$$

Air transportation, rail transportation and waterway transportation, add up to a large amount of greenhouse gas emissions, of which aviation accounts for a small proportion, because people rarely need long-distance transportation in their daily lives. However, because aircraft emissions are at high altitudes, which directly affects the climate environment, coupled with the rapid growth of the aviation industry, it means that aircraft will become a major source of global warming[17].

5.3 Water pollution in aviation

The wastewater discharged from the airport includes the following aspects:

- Industrial wastewater
- Surface runoff wastewater
- Domestic wastewater

One of the greatest threats to water resources is airport runoff, which includes airport washing areas, hangars, fuel and lubricant storage areas.

Major components of airport runoff:

- liquid fossil fuels such as petroleum
- various disinfectants and cleaning agents
- de-icers used in airports
- spent electrolytes from batteries
- various solvents

With the increase of urban population and the development of urban population and the development of industrial and agricultural production the discharge of sewage is also increasing, and the water pollution is quite serious, it is almost all over the world. Statistics show that at the end of 2000 , about 300 of the 663 cities in China had sewage treatment facilities. The annual sewage treatment volume was 11.36 billion cubic meters, but the wastewater treatment rate was only 34.2% [16].

It is very important to purify water. If it is used for drinking water, it must not contain substances that are harmful to human health.

Biological water treatment can be divided into 3 categories:

1. Aerobic process (bacteria degrade organic matter and convert it into CO₂, which can be used by plants for their growth).

2. Anaerobic process (is used to ferment the sludge or waste at a specific temperature, oxygen isn't used).

3. Composting (type of aerobic process in which in the presence of oxygen the sludge is mixed with sawdust or other carbon sources).

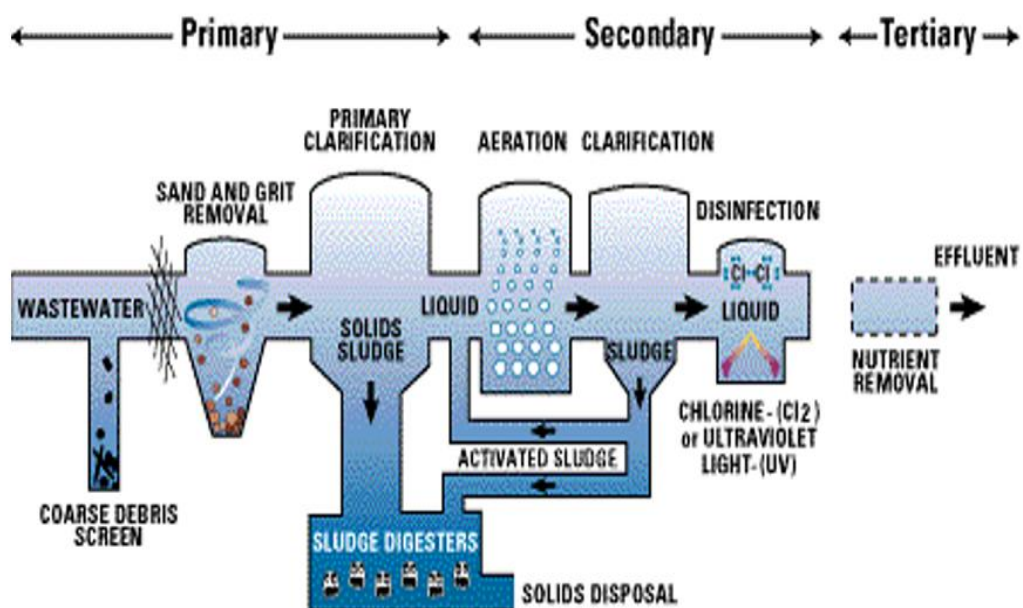


Fig 5.1 scheme of wastewater treatment

5.4 Acoustic (noise) pollution

Noise pollution is no less serious than air and water pollution. Noise is a sound with a very chaotic frequency and intensity, and seen as a loud disturbance. Noise can damage the balance of the human body. Noise is generated due to mechanical vibrations of elastic media such as solids, liquids and gases, but such oscillations are non-periodic and random[18].

Types of noise:

- Vibration during operation of mechanical equipment
- hydraulic shock, turbulence and other liquid processes
- air flowing through pipes
- magnetic field fluctuations of some electromechanical facilities

Sources of noise pollution at airport:

- Activation of the aircraft power units (PU) and auxiliary power units (APU).
- Mechanical, thermal machines and wind turbines used in various airport services.
- Manufacture of machinery.

Noise can affect people's hearing and nervous system. Being in a noisy environment for a long time will reduce people's ability to respond, and they will also become emotionally unstable, easily depressed and even angered.

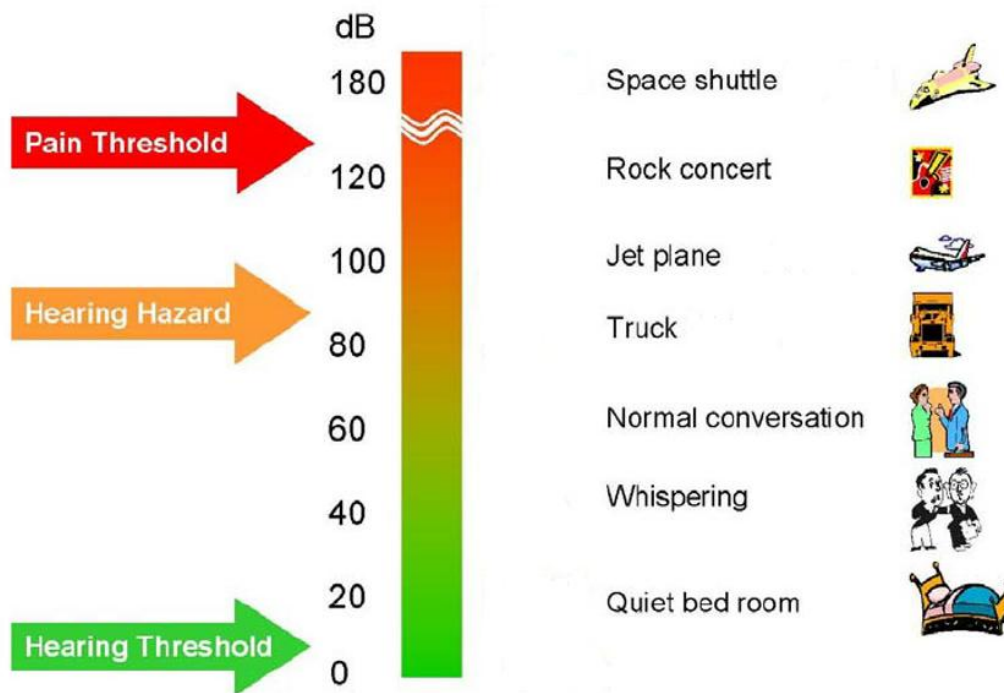


Fig 5.2 The division of sound decibels

The picture 5.3 below is the acute, chronic, long-term effect of noise

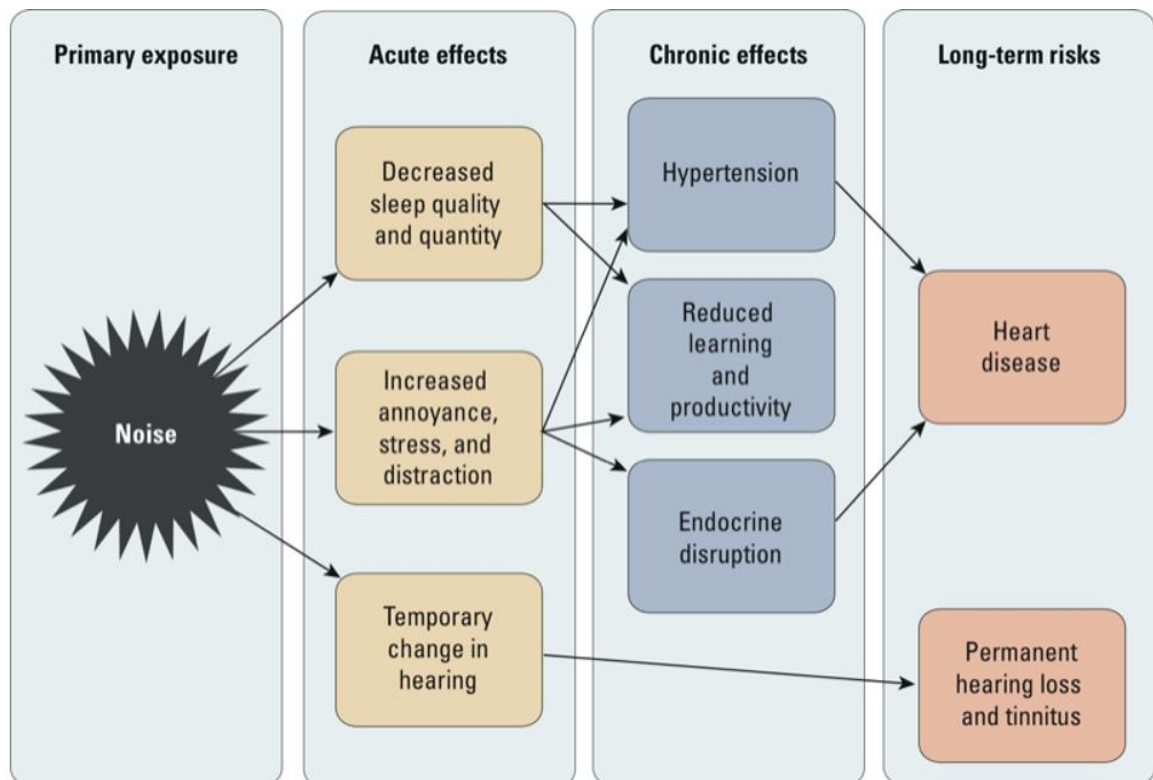


Fig 5.3 The gradual effect of noise

5.5 Soil contamination

Contamination have local character and is associated with both liquid spills and emissions of particulate and gaseous toxic substances deposited on the surface of the soil. Erosion and soil pollution areas near the airfield is due to the flooding of sewage from artificial coatings and waterproof soil [17].

Amount of land pollution damage (L_p) is given by:

$$L_p = A \cdot S_c \cdot M_p \cdot C_p \cdot C_{hp} \cdot C_e$$

A - specific costs for land pollution liquidation, the value of which is equal to 0.5

S_c - contaminated land area, m^2

M_p - normative monetary value of polluted land, hrn/m^2

C_p - coefficient of land pollution, characterizes input pollutants into the contaminated land capacity, depending on the depth of infiltration

C_{hp} - coefficient of hazardous pollutant (Table 5.1)

C_e - environmentally-economic value of land (Table 5.2).

The land pollution coefficient (C_p) is determined by the concentration of pollutants due to the formula:

$$C_p = C_{ps} \cdot D / (D_{0.2} \cdot I \cdot C_{calc})$$

C_{ps} - the concentration of polluting substance due to instrumentally-laboratory monitoring, mg/kg

D - depth of infiltrated with pollutants land layer, m

$D_{0.2}$ - depth of land layer, that is the dimensional unit for calculating the costs for land pollution liquidation depending on the depth of infiltration and equals 0.2 m

I - correction index for the costs for land pollution liquidation depending on the depth of infiltration of pollutants (Table 5.3)

C_{calc} - calculated coefficient is equal to 1000000 mg/kg.

Amount of land damage littered with rubbish (L_r) is given by:

$$L_r = A \cdot B \cdot M_r \cdot S_r \cdot C_r \cdot C_{hw} \cdot C_e$$

where A - specific costs for land pollution liquidation, the value of which is equal to 0.5

B - conversion coefficient equals 10 (contaminated with domestic and industrial waste) and equals 100 (with dangerous (toxic) waste)

S_r - littered with rubbish land area, m²

M_r - normative monetary value of littered with rubbish land, hrn/m²

C_r - coefficient of littered with rubbish land, characterizes the degree of contamination by waste (Table 5.4);

C_{hw} - coefficient of hazardous waste (Table 5.5);

C_e - environmentally-economic value of land (Table 5.2).

Table 5.1 Coefficients of hazardous pollutant (C_{hp})

Group of danger	Dangerous level	Polluting substances (values of measurements) referred to group of danger	C_{hp}
I	extremely dangerous (maximum allowable concentration < 0.2 mg/kg)	Oil, oil products, lead	4.0
II	highly dangerous (maximum allowable concentration 0.2-0.5 mg/kg)	Cobalt, copper, molybdenum, chromium	3.0
II	moderately dangerous (maximum allowable concentration > 0.5 mg/kg)	Anionic surface-active agents (ASAA), manganese, nitrates	2.5
IV	Other (maximum allowable concentrations aren't determined)	Ammonium, chlorides	1.5

Table 5.2 Scale of environmentally-economic value of lands

Categories of lands and lands under special protection	C_e
Lands of sanitary protection zones around facilities with open and underground water supply sources, water intake and water treatment plants, water pipes, coastal protection strips along the seas, rivers and around water	5.5
Health-related lands	5.0
Nature reserve and other environmental purposes lands	4.5
Recreational lands	4.0
Agricultural lands	1.0

Table 5.3 Depth of infiltration correction index (I)

Depth of infiltration, m	I	Depth of infiltration, m	I
0-0.2	0.100	0-1.2	0.049
0-0.4	0.082	0-1.4	0.044
0-0.6	0.070	0-1.6	0.040
0-0.8	0.060	0-1.8	0.037
0-1.0	0.054	0-2.0	0.033

Table 5.4 Littered with rubbish lands coefficients (C_r)

Contamination level	Waste volume, m ³	C_r
1	0-5	1.25
2	5-10	1.50
3	10-20	2.00
4	20-50	2.50
5	50-100	3.00
6	Above 100	4.00

Table 5.5 Hazardous waste coefficients (C_{hw})

Dangerous class	Danger level	C_{hw}
I	extreme dangerous	3.0
II	high dangerous	2.0
II	moderate dangerous	1.5
IV	low dangerous	1.0

5.6 Calculation of CO and NO_x emissions by aircraft

Aircrafts pollute the atmosphere as a result of emission of detrimental compounds with discharge gases of aircraft engines. Emissions of CO and NO_x at the airport zone are calculated for takeoff and landing cycle [17]. Characteristics of regimes and their duration are given in table 5.6.

Table 5.6

Number of regime	Characteristics of regimes	Relative thrust \bar{R}	Duration of regime t, min
1	Start, idle running before takeoff (regime of low gas)	0.07	15.0
2	Takeoff	1.0	0.7
3	Climb	0.85	2.2
4	Approach landing from a height of 1000 m	0.42	4.0
5	From landing taxiing (regime of low gas)	0.07	7.0

Calculations of emissions of CO and NO_x from aircraft engine are based on formulas:

$$M_{CO} = M_{CO\ GO} + M_{CO\ TLO}, \text{ kg}$$

$$M_{NO_x} = M_{NO_x\ GO} + M_{NO_x\ TLO}, \text{ kg}$$

where $M_{CO\ GO}$, $M_{NO_x\ GO}$ - masses of CO and NO_x , which are emitted during ground operations (start, idle running, from landing taxiing – regime 1 and 5); $M_{CO\ TLO}$, $M_{NO_x\ TLO}$ - masses of CO and NO_x respectively, which are emitted during takeoff and landing operations (takeoff, climb to 1000 m, approach landing from a height of 1000 m – regimes 2, 3, 4).

$$M_{CO\ GO} = K_{CO} \cdot C_{SP\ LG} \cdot R_{LG} \cdot T_{LG}, \text{ kg}$$

$$M_{NO_x\ GO} = K_{NO_x} \cdot C_{SP\ LG} \cdot R_{LG} \cdot T_{LG}, \text{ kg}$$

where K_{CO} , K_{NO_x} – emission indexes of CO and NO_x relatively during ground operations (table 5.7); $C_{SP\ LG}$ – specific consumption of fuel during regime of low gas, $\text{kg}/\text{N}\cdot\text{h}$; R_{LG} – engine thrust at low gas, $R_{LG} = \bar{R} \cdot R_0$, N , \bar{R} – relative thrust, R_0 – maximal thrust of engine, N ; T_{LG} – operating time of engine at low gas for one takeoff and landing cycle (regimes 1 and 5), hour.

Table 5.7

Ingredients	CO	NO _x
Coefficient of released substances K (kg of ingredient/kg of fuel)	0.0546	0.0054

Calculations of CO and NO_x emissions during takeoff and landing operations (regimes 2, 3, 4) are based on formula:

$$M_{CO\ TLO} = W_{CO\ T} \cdot T_T + W_{CO\ C} \cdot T_C + W_{CO\ L} \cdot T_L, \text{ kg}$$

$$M_{NO_x\ TLO} = W_{NO_x\ T} \cdot T_T + W_{NO_x\ C} \cdot T_C + W_{NO_x\ L} \cdot T_L, \text{ kg}$$

where $W_{CO\ T}$, $W_{NO_x\ T}$ – weight rate of CO and NO_x emissions relatively during aircraft takeoff, kg/hour; $W_{CO\ C}$, $W_{NO_x\ C}$ – weight rate of CO and NO_x emissions relatively during climb to 1000 m; $W_{CO\ L}$, $W_{NO_x\ L}$ – weight rate of CO and NO_x emissions relatively during Approach landing from a height of 1000 m (table 5.8); T_T , T_C , T_L – operating time of engine during takeoff, climb to 1000 m and descent from 1000 m relatively (table 5.6).

Table 5.8

Regimes	weight rate emission, kg/h		
	CO	C _x H _y	NO _x
Takeoff	6	2.5	89
Climb	8.8	2.5	53
Decline from 1000m	16	2.8	16

$T_1 = 0.7 \text{ min} = 0.0117 \text{ hour}$ - time during takeoff;

$T_2 = 2.2 \text{ min} = 0.0367 \text{ hour}$ - during climb;

$T_3 = 4.0 \text{ min} = 0.0667 \text{ hour}$ - decline.

We put the above data into the corresponding formula to get the following results:

$$M_{CO} = 0.0546 \times 0.065 \times 7.2 \times 1000 \times 0.367 + 6 \times 0.0117 + 8.8 \times 0.0367 + 16 \times 0.0667 = 9.377 + 1.46 = 10.837 \text{ (kg)} = 10837 \text{ (g)}$$

$$M_{NO_x} = 0.0054 \times 7.2 \times 1000 \times 0.065 \times 0.367 + 89 \times 0.0117 + 53 \times 0.0367 + 16 \times 0.0667 = 0.9275 + 4.0536 = 4.981 \text{ (kg)} = 4981 \text{ (g)}$$

$$\frac{M_{CO}}{R_0} = \frac{10837}{103} = 105.2g / \kappa N$$

$$\frac{M_{NOx}}{R_0} = \frac{4981}{103} = 48.4g / \kappa N$$

Compared with the criteria mentioned in the previous section 5.2 we know that it fits the emission standards stipulated by ICAO.

5.7 Biofuels

The official definition : biofuels - any fuel that contains (by volume) no less than 80% of materials got from living organisms and collected in 10 years before production.

Raw materials for the production of biofuels can be varied oil plants. Such as canola, palm, coconut, soybean oils.

The advantages of biofuel is the lack of sulfur in the composition of the exhaust gases, and consequently that such biofuels don't lose lubricating properties, so that the engine can serve much longer[19].

Conclusion

The economy is developing rapidly, and we also need to see the resource and environmental problems behind it. Effective management of airport energy can greatly promote sustainable development. Not only airports but everyone of us can make a contribution to environmental protection.

Chapter 6 FUEL CONSUMPTION REDUCTION WITH MICRO-CIRCUIT METHOD

Engine designers have been thinking for years about how to cool the tips of turbine blades more efficiently. Because this can extend the life of the blades and save more costs. Not only can this be achieved if the cooling gas is used more efficiently when cooling the blades, it can also improve the efficiency of the engine.

Based on the patent No. US 2004/0151587A1 , We can learn about a new cooling method - micro-circuit cooling[20].

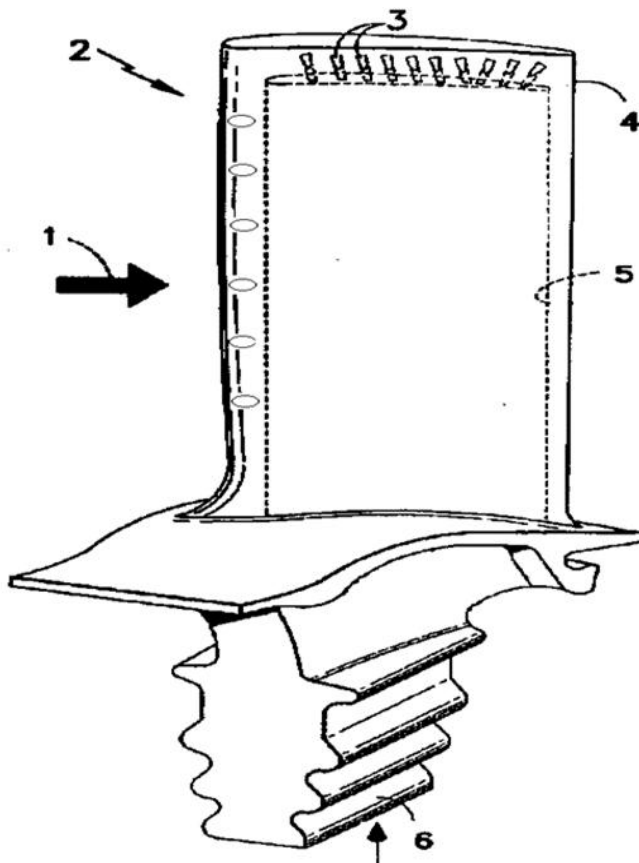


Fig.6.1 Traditional cooling

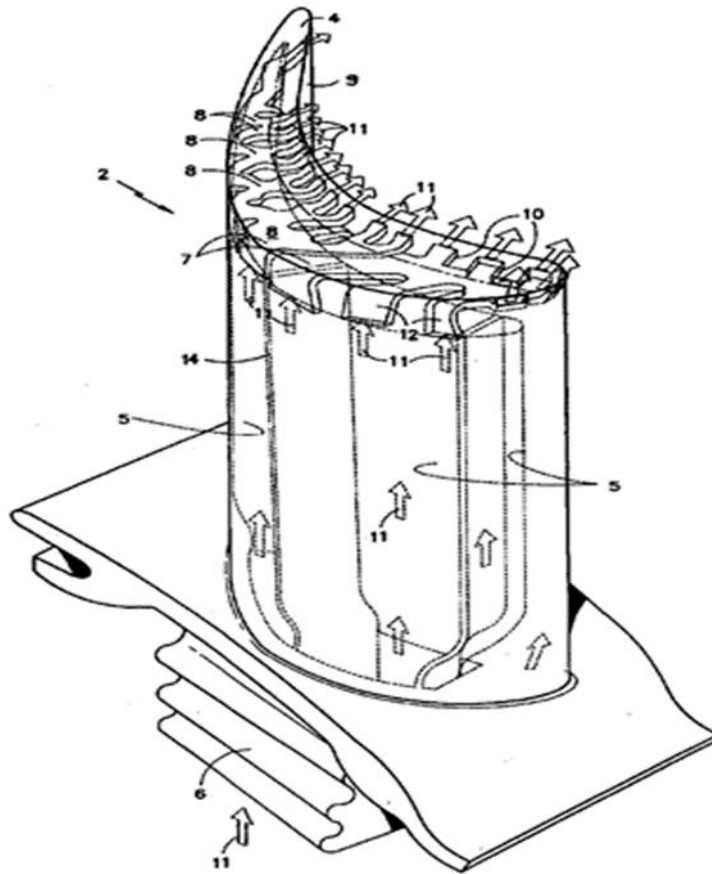


Fig 6.2 Microcircuit cooling in blades

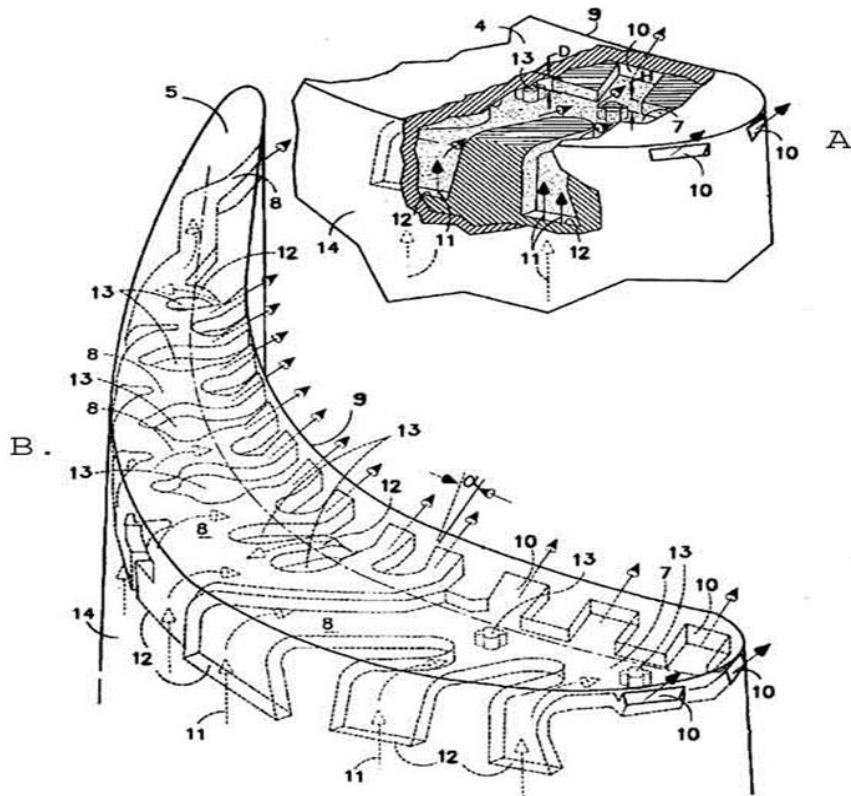


Fig.6.3 Picture of blade flank fragment

It can be seen from the figure that the new cooling method has many entry places 12 and outlets 10 connected to the cavity 7, and the cooling gas 11 enters the cavity 5 through 12 into 7 and finally exits from 10.

Comparing it with the traditional cooling method, it can be found that its improvement is that the cooling gas will hit the blade tip 4 when it passes 12, and we know that a vortex will be generated around the blade tip. This is more effective to achieve the purpose of cooling.

The cooling air 11 is accelerated into the micro channels 8, thereby increasing the efficiency of heat exchange and cooling of the blade surface. Conventional methods focus on the integral formation of a cooling air film on the leading edge. It results in an increase in effective blade thickness and a decrease in turbine efficiency. The proposed design will only form a cooling film at the tip where it is most needed, so the overall blade effective thickness will increase slightly. Additionally, cooling air flowing to the tip will keep the airflow overflowing over the tip, resulting in some impact on turbine efficiency positive influence.

6.1 Quantitative analysis of the influence of g_{cool} on C_{sp}

Supposing that turbine efficiency is constant $\eta_T^*=0.9$, $g_{cool}=0.08$, $C_{sp}=0.03789 \text{ Kg/N}\cdot\text{h}$, $\eta_\varepsilon=0.341$

Reducing g_{cool} at 5%, $g_{cool}=0.03$

Calculation holds in ground conditions at normal ambient conditions $V=0 \text{ m/s}$, $T_H=288\text{K}$, $P_H=101325\text{Pa}$

total pressure p_{am}^* and total temperature T_{am}^* for flight altitude H :

$$T_{am}^* = T_{am} + \frac{k-1}{k} \frac{V^2}{2R} = 288 \text{ K}$$

$$p_{am}^* = p_{am} \left(\frac{T_{am}^*}{T_{am}} \right)^{\frac{k-1}{k}} = 1.013 \cdot 10^5 \text{ Pa}$$

At the entry to the fan:

The total air temperature $T_{fi}^* = T_{am}^* = 288 \text{ K}$

$$p_{fi}^* = p_{am}^* \cdot \sigma_i = 1.013 \cdot 10^5 \cdot 0.99 = 1 \cdot 10^5$$

Where total pressure recovery coefficient in the inlet $\sigma_i=0.99$

Behind the fan:

fan efficiency $\eta_{fani} = 0.91$

work of air compression in the fan:

$$L_{fanII} = \frac{k}{k-1} RT_{fi}^* \left(\pi_{fanII}^{*\frac{k-1}{k}} - 1 \right) \frac{1}{\eta_{fanII}^*}$$

$$L_{fanII} = \frac{1.4}{1.4-1} \cdot 287 \cdot 288 \cdot (1.65^{0.286} - 1) \cdot \frac{1}{0.91} = 45.7 \frac{\text{kJ}}{\text{kg}}$$

total air temperature:

$$T_{fdII}^* = T_{fi}^* + \frac{k-1}{k} \frac{L_{fanII}}{R} = 288 + \frac{1.4-1}{1.4} \cdot \frac{45700}{287.3} = 333.5 \approx 334 \text{ K}$$

total air pressure:

$$p_{fdII}^* = p_{fi}^* \cdot \pi_f^* = 1 \cdot 10^5 \cdot 1.6 = 1.60 \cdot 10^5 \text{ Pa}$$

At the exit from the secondary flow jet nozzle:

total air temperature $T_{jnII}^* = T_{fdII}^* = 334 \text{ K}$

total air pressure before the jet nozzle:

$$p_{jnII}^* = p_{jdII}^* \cdot \sigma_{sf} = 1.6 \cdot 10^5 \cdot 0.995 = 1.59 \cdot 10^5 \text{ Pa}$$

Where recovery coefficient $\sigma_{sf} = 0.995$

jet nozzle pressure ratio $\frac{p_{jnII}^*}{p_{am}^*} = \frac{1.6}{1.013} = 1.576$, accepting $\varphi_{jnII} = 0.98$

$$c_{jnII} = \varphi_{jnII} \sqrt{2 \cdot \frac{k}{k-1} \cdot RT_{jnII}^* \left(1 - \left(\frac{p_{am}^*}{p_{jnII}^*} \right)^{\frac{k-1}{k}} \right)}$$

$$c_{jnII} = 0.98 \cdot \sqrt{2 \cdot 3.5 \cdot 287 \cdot 334 \cdot \left(1 - \left(\frac{1.013}{1.6} \right)^{0.286} \right)} = 280.2$$

$$\approx 280 \text{ m/s}$$

Behind the compressor:

Set compressor stage efficiency $\eta_{st}^* = 0.9$

compressor efficiency:

$$\eta_c^* = \frac{\pi_c^{*\frac{k-1}{k}} - 1}{\pi_c^{*k\eta_{st}^*} - 1} = \frac{32^{0.286} - 1}{32^{\frac{0.286}{0.9}} - 1} = 0.8438 \approx 0.84$$

work of air compression in the compressor:

$$L_c = \frac{k}{k-1} \cdot RT_{ci}^* \left(\pi_c^{*\frac{k-1}{k}} - 1 \right) \frac{1}{\eta_c^*}$$
$$L_c = 3.5 \cdot 287 \cdot 288 \cdot (32^{0.286} - 1) \cdot \frac{1}{0.84} = 580.61 \approx 581 \text{ KJ/Kg}$$

The total air temperature behind the compressor:

$$T_{cd}^* = T_{ci}^* + \frac{k-1}{k} \frac{L_c}{R} = 288 + 0.286 \cdot \frac{581000}{287} = 865.4 \approx 865 \text{ K}$$

The total air pressure behind the compressor:

$$P_{cd}^* = p_{ci}^* \pi_c^* = 1 \cdot 10^5 \cdot 32 = 32 \cdot 10^5 \text{ Pa}$$

Behind the combustion chamber:

Set total pressure recovery coefficient in the combustion chamber $\sigma_{cc} = 0.98$, the total air pressure before the turbine:

$$P_{ti}^* = P_{cd}^* \sigma_{cc} = 32 \cdot 10^5 \cdot 0.98 = 31.45 \cdot 10^5 \approx 31.5 \cdot 10^5 \text{ Pa}$$

The turbine inlet temperature $T_{ti}^* = 1500 \text{ K}$

The average specific heat of gas in the combustion chamber:

$$\bar{c}_p = 878 + 0.208 \cdot (T_{ti}^* + 0.48T_{cd}^*)$$
$$\bar{c}_p = 878 + 0.208 \cdot (1500 + 0.48 \cdot 865) = 1287 \frac{\text{J}}{\text{kg} \cdot \text{K}}$$

Set combustion efficiency $\eta_{cc} = 0.99$ and net calorific value of fuel

$$H_u = 43000 \text{ kJ/kg}$$

relative fuel consumption:

$$g_f = \frac{\bar{c}_p(T_{ti}^* - T_{cd}^*)}{\eta_{cc}H_u} = \frac{1287 \cdot (1500 - 865)}{0.99 \cdot 43 \cdot 10^6} = 0.0207$$

Behind the turbine:

mechanical efficiency $\eta_m = 0.99$

effective work of all stages of the turbine:

$$L_t = \frac{mL_{fanII} + L_c}{(1 + g_f)(1 - g_{cool})\eta_m}$$

$$L_t = \frac{5 \cdot 45.7 + 581}{(1 + 0.0207) \cdot (1 - 0.06) \cdot 0.99} = 825.67 \approx 826 \text{ KJ/Kg}$$

Set turbine efficiency $\eta_t^* = 0.91$

the turbine outlet temperature and turbine outlet pressure:

$$T_{td}^* = T_{ti}^* - \frac{k_g - 1}{k_g} \cdot \frac{L_t}{R_g} = 1500 - \frac{1.33 - 1}{1.33} \cdot \frac{826000}{288} = 839 \text{ K}$$

$$p_{td}^* = p_{ti}^* \left(1 - \frac{T_{ti}^* - T_{td}^*}{T_{ti}^* \eta_t^*}\right)^{\frac{k_g}{k_g - 1}}$$

$$p_{td}^* = 31.5 \cdot 10^6 \cdot \left(1 - \frac{1500 - 839}{1500 \cdot 0.91}\right)^4 = 1.86 \cdot 10^5 \text{ Pa}$$

At the exit from the primary flow jet nozzle:

$$T_{jnI} = T_{td}^* = 839 \text{ K}$$

Set recovery coefficient $\sigma_{jnI} = 0.98$

total air pressure at the exit from the primary flow jet nozzle:

$$p_{jnI} = p_{td}^* \cdot \sigma_{jnI} = 1.86 \cdot 10^5 \cdot 0.98 = 1.82 \cdot 10^5 \text{ Pa}$$

jet nozzle pressure ratio of the primary flow and critical pressure ratio at the jet nozzle:

$$\pi_{jnI} = \frac{p_{jnI}}{p_{am}} = \frac{1.798}{1.013} = 1.80$$

$$\pi_{jn_{cr}} = \left(\frac{k_g + 1}{2}\right)^{\frac{k_g}{k_g - 1}} = \left(\frac{1.33 + 1}{2}\right)^4 = 1.85$$

$\pi_{jn_I} < \pi_{jn_{cr}}$, full expansion takes place in the jet nozzle of the engine
primary flow $p_{jn_I} = p_{am}$

$$c_{jn_I} = \varphi_{jn_I} \sqrt{2 \cdot \frac{k_g}{k_g - 1} \cdot R_g T_{td}^* \left(1 - \left(\frac{p_{am}}{p_{td}^*} \right)^{\frac{k_g - 1}{k_g}} \right)}$$

$$c_{jn_I} = 0.98 \cdot \sqrt{2 \cdot 4 \cdot 288 \cdot 839 \cdot \left(1 - \left(\frac{1.013}{1.86} \right)^{0.25} \right)} = 511.3 \text{ m/s}$$

The static air temperature:

$$T_{jn_I} = T_{td}^* - \frac{k_g - 1}{k_g} \cdot \frac{c_{jn_I}^2}{2R_g} = 839 - \frac{0.33 \cdot 511^2}{1.33 \cdot 2 \cdot 288} = 726 \text{ K}$$

6.2 Main specific parameters and mass flow rate calculation

Specific thrust of the primary flow:

$$P_{spI} = c_{jn_I} (1 + g_f) = 511 \cdot (1 + 0.0207) = 522 \frac{\text{N} \cdot \text{s}}{\text{kg}}$$

Specific thrust of the secondary flow:

$$P_{spII} = c_{jn_{II}} = 280 \frac{\text{N} \cdot \text{s}}{\text{kg}}$$

Specific thrust of turbofan engine without mixing flows:

$$P_{sp} = \frac{P_{spI} + mP_{spII}}{1 + m} = \frac{522 + 5 \cdot 280}{1 + 5} = 320.47 \approx 320 \frac{\text{N} \cdot \text{s}}{\text{kg}}$$

The specific fuel consumption:

$$C_{sp} = \frac{3600 \cdot g_f (1 - g_{cool})}{P_{sp} (1 + m)} = \frac{3600 \cdot 0.0207 \cdot 0.97}{320 \cdot (1 + 5)} = 0.03758 \frac{\text{kg}}{\text{N} \cdot \text{h}}$$

The total mass air flow rate G_a , the mass flow rate through the inner duct G_{aI} and through the outer duct G_{aII} :

$$G_{aI} = \frac{G_a}{1 + m} = \frac{374.4}{1 + 5} = 62.4 \text{ kg/s}$$

$$G_{aII} = \frac{m}{1+m} \cdot G_a = \frac{5}{1+5} \cdot 157 = 312.0 \text{ kg/s}$$

$$G_a = G_{aI} + G_{aII}$$

$$G_a = \frac{P}{P_{sp}} = \frac{120000}{320} = 374.4 \text{ kg/s}$$

The internal engine efficiency:

$$\eta_{in} = \frac{P_{spI}^2 + mP_{spII}^2}{2g_f H_u (1 - g_{cool})} = \frac{522^2 + 5 \cdot 280^2}{2 \cdot 0.0207 \cdot 43 \cdot 10^6 \cdot (1 - 0.03)} = 0.385$$

Conclusions

Micro-circuit cooling method based on the patent can finally increase the fuel consumption efficiency:

We decrease g_{cool} 5% from 0.08 to 0.03.

Then we can get:

(1) Improved engine internal efficiency η_e from 0.341 to 0.385

(2) Improved engine turbine efficiency from 0.9 to 0.91

(3) Decreased specific fuel consumption from $C_{sp}=0.03758 \text{ Kg/N}\cdot\text{h}$ to $C_{sp}=0.03789 \text{ Kg/N}\cdot\text{h}$.

Chapter 7 ANALYSIS OF ENGINE FUEL SYSTEM

The engine fuel systems serve for indispensable fuel supply from aircraft fuel system to the engine combustion chamber in most useful kind for its complete combustion. They also supply fuel (as working fluid) to hydro-mechanisms of automatic control systems and (as cooling liquid) to fuel-oil coolers.

Fuel feeding system has three main lines:

- low pressure;
- high pressure;
- starting fuel.

It also contains fuel drain system.

7.1 Fuel delivery system

Fuel from the aircraft fuel supply system enters the engine at the fuel pump inlet.

The fuel is pressurized through the LP stage of the fuel pump and flows through the main oil/fuel heat exchanger and the fuel filter.

The fuel then flows through the HP stage of the pump, through the wash filter and enters the Main Engine Control(MEC).

Since the fuel pump has a higher fuel flow capacity than the fuel and control system requires, the fuel flow is divided in the MEC into metered flow and bypass flow.

Bypass fuel is ported back to the outlet of the fuel pump LP stage.

Metered fuel from the MEC flows through the pressurizing valve, the flowmeter, the fuel manifold, and fuel nozzles into the combustion

chamber.

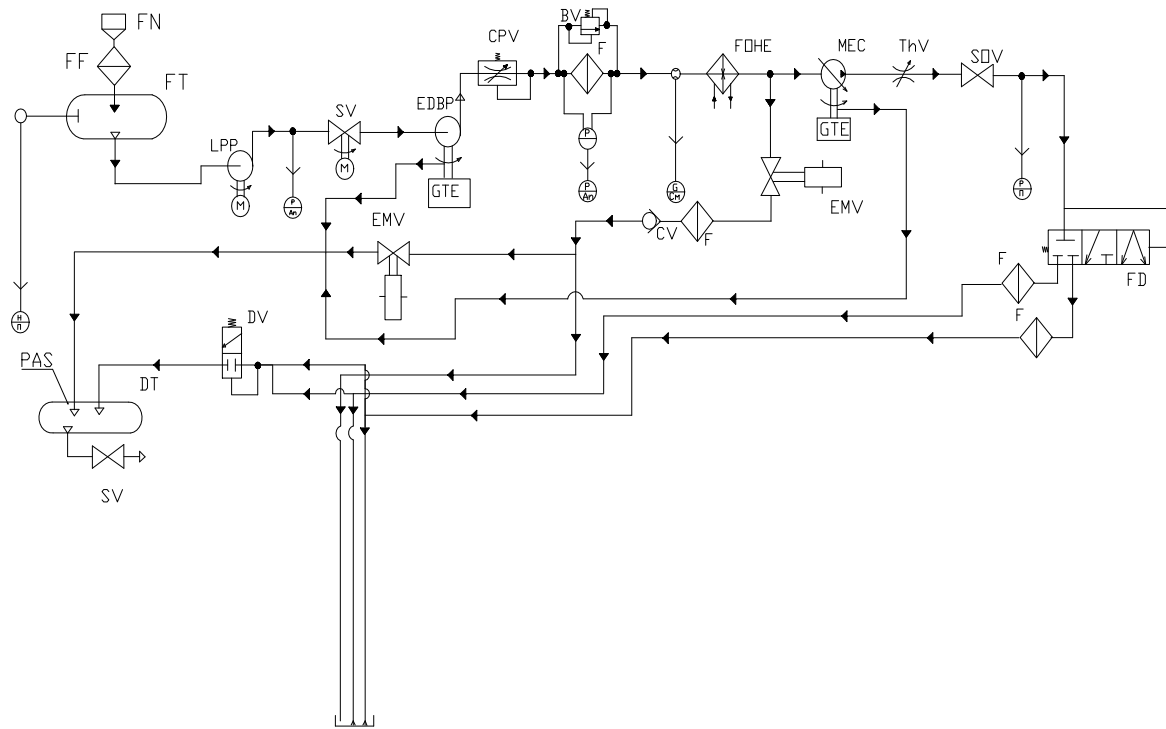


Fig.7.1 Fuel delivery system

FN—fill neck; FT—fuel tank; FF—fuel filter; LPP—low pressure pump;
M—motor; SV—safety valve; EDBP—engine driven backup(booster)
pump; GTE—gas turbine engine; CPV—constant pressure valve;
BV—bypass valve; FOHE—fuel oil heat exchanger; CV—check valve;
MEC—main engine control; ThV—throttle valve; SOV—shut off valve;
EMV—electric magnetic valve; FD—fuel distributor; DV—drainage valve;
DT—drainage tank; PAS—pressurized air supply; P_f —fuel pressure;
 ΔP —fuel pressure differetial; H_f —fuel level; G_f —fuel consumption;
 S_g —signal

7.2 Automatic fuel control system

The automatic control system of projected engine is established based on principle of deviation. The controlled value is measured, and has an influence on the controlled object, which depends on given deviation and controlled parameter. Apparently, the controlled value can not be supported totally exact, as only its deviation from the given value causes the controlling influence on the controlled object. Relation between the controlled object and regulator is negative feed-back, and principle of controlling is closed.

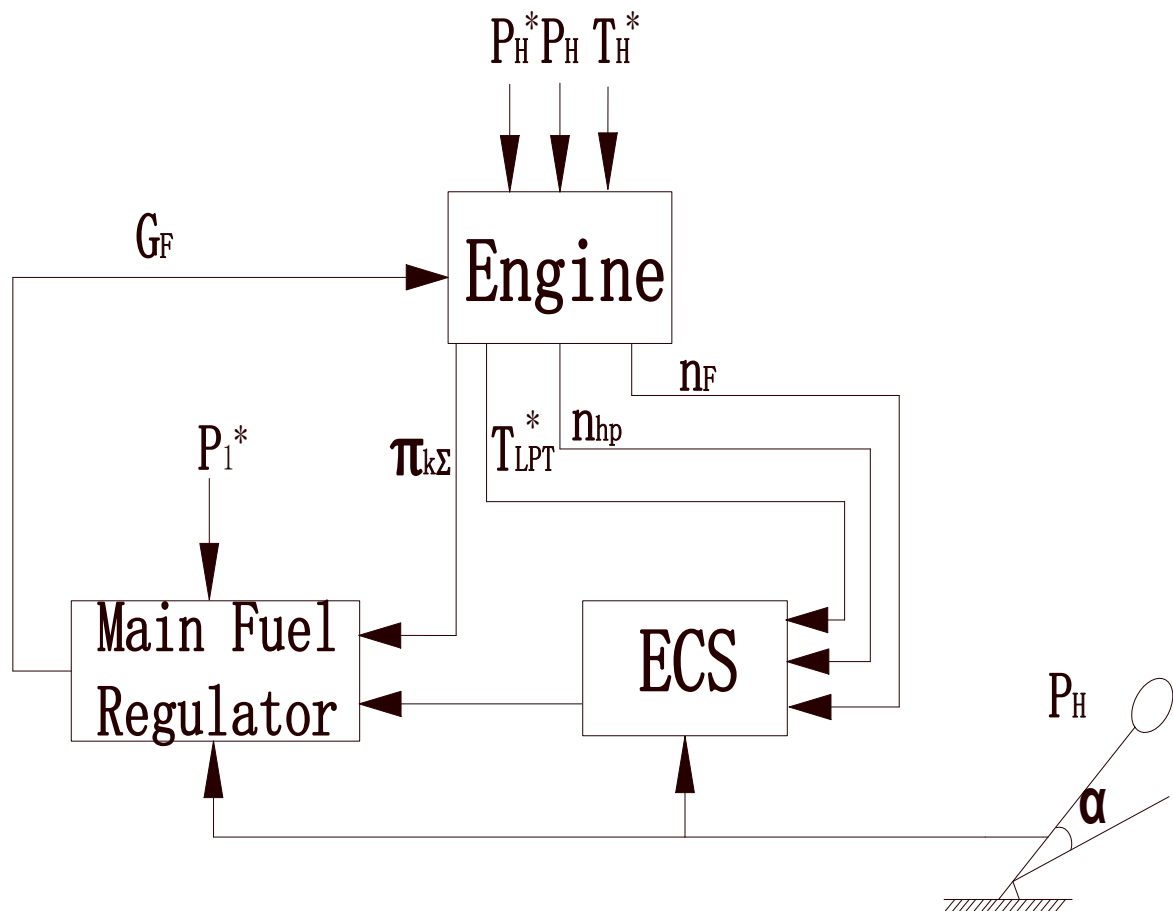


Fig.7.2 Block diagram of fuel ACS

Basic controlled value is $\pi_{K\Sigma}$. It is measured and compared in a regulator with a size which specified by position of TCL. Differences between two indicated values causes the change of control factor—fuel flow rate G_f . The parameter $\pi_{K\Sigma}$ is corrected according to P_1^* .

Other controlled values (T_{LP}^* , n_{HP} , n_F) are regulated entering in the special device, electronic control system (ECS). Here takes place their comparison with the values, which is set by the system. T_{LP}^* is variable and depends on position of TCL, n_{HP} and n_F is constant on all modes of operations of engine, ECS provides the choice of parameter on which a controlling is conducted: on the steady modes it is chosen one controlled parameter from the three which provides the minimal delivery of fuel.

GENERAL CONCLUSIONS

(1) Improving the fuel efficiency of aircraft has always been a topic of research, which is of great help to today's society. There are three main improvements:

- aerodynamic improvements
- engine performance improvements
- improved aircraft configuration.

(2) In this diploma result, the improvement of engine fuel efficiency is stated in the first part, some of the improvement methods are as follows:

- increase the parameters of working processes (overall pressure ratio, bypass ratio, turbine inlet gas temperature, etc).
- improve efficiency of engine units (compressor, turbine, combustor).
- reduction of compressed air taken from compressor for different service purposes inside of engine.

(3) Parameters of working process chosen for the projected engine Bypass ratio $m= 5$, Compressor pressure ratio $\pi= 30$, Temperature of a gas entering turbine $T_g= 1500$ K. We calculate specific engine fuel consumption $C_{sp} = 0.0376$ Kg/N·h, which corresponds to the modern level of aviation turbofan engine development.

(4) In development of the projected engine assemblies construction, CFM-56 was taken as prototype, because this engine meets most of modern demands introduced to TFE.

(5) Microcircuit cooling method of turbine blades developed by US

scientists Frank K. and Bryan D. allows to optimize engine performance by reducing amount of air bleed for turbine blades cooling, increasing efficiency of turbine , and decreasing specific fuel consumption.

(6) In the chapter of labor protection, measures to reduce the impact of dangerous and harmful factors on workers are proposed, and OSH (Occupational Safety and Health) standards are also proposed.

(7) In the environmental protection chapter, the emission of the aircraft is calculated, the result is in line with the emission standards, some suggestions are put forward, such as using some bio-alternative fuels.

REFERENCES

1. Study on effective parameter of the triple-pressure reheat combined cycle performance, Prof. Dr. Md. Mustafizur Rahman - Oct 2012.
2. Variation of thermal efficiency with TET, Barinyima Nkoi - Dec 2013.
3. Future Airplane Fuel Efficiency- QINETIQ/10/00473. March, 2010.
4. Turbofan operation, K. Aainsqatsi - 6 May 2008.
5. Investigation of the efficiency limits of the traditional gas turbine engines, Evgeny Filinov, Andrey Tkachenko, Yaroslav Ostapyuk, Ilia Krupenich - Jan 2017.
6. JOURNAL OF PROPULSION AND POWER; Vol. 17, No. 5, September–October 2001 “Optimum Fan Pressure Ratio for Bypass Engines with Separate or Mixed Exhaust Streams” Abhijit Guha University of Bristol, Bristol, England BS8 1TR, United Kingdom.
7. Design and strength of aircraft engines: Thermodynamic and gas-dynamic calculation for aircraft gas turbine engines-Methodical guide for writing the course paper./ V.V Yakimenko, L.G Volyanska, V.V Panin, I.I Gvozdetsky. Kiev NAU, 2003.
8. Design and strength of aircraft engines: Method guide for performing computation and design work and homework-GTE turbine rotor blade strength calculation./ S.I. Yovenko, I.I.Gvozdetsky,O.I.Chumak, Kyiv NAU,2007.
9. calculations for Ni-based superalloys. N.Saunders,Thermotech Ltd,

The University of Birmingham Edgbaston, Birmingham B15 2TT,
U.K.1996.

10. Annex 16 to the Convention on International Civil Aviation. Volume 1.
Aircraft noise. Third edition - July 1993.

11. O.S. Protoiereiskiy, O.I. Zaporozhets. Basics of labour protection.
Education manual – K: NAU, 2002.

12. O.S. Protoiereiskiy, O.I. Zaporozhets. Branch labour precaution NAU
2005-286c.

13. ICAO Doc. 9137 Airport Services Manual(ASM)- Part 1- Rescue and
Fire Fighting - November 2018.

14. OSH-Standards-2020-Edition.pdf - 34p.


15. ICAO annex 14 volumes for the norm of safety management system in
civil aviation.

16. 知乎专栏 机场生活污水处理

<https://zhuanlan.zhihu.com/p/345991622>

17. Guidelines for the implementation of the section of the diploma work
"Environmental Protection" for students of specialties 1610, 1610BI, 121
3, 1611. Kiev: KIIGA. 1987.

18. ICAO exhaust emissions data bank. 1st edition. -Montreal, 1995.

19. "Biofuels - Types of Biofuels - Bioethers".  biofuel.org.uk. Archive
d from the original on 1 February 2016.

20. US patent No: US 2004/0151587A1. Microcircuit cooling for a turbine
blade tip, 2004